Journal of Vertebrate Paleontology 34(5):1133–1154, September 2014
© 2014 by the Society of Vertebrate Paleontology

ARTICLE

THE BASAL TITANOSAURIAN *RUKWATITAN BISEPULTUS* (DINOSAURIA, SAUROPODA) FROM THE MIDDLE CRETACEOUS GALULA FORMATION, RUKWA RIFT BASIN, SOUTHWESTERN TANZANIA

ERIC GORSCAK,[1,2] PATRICK M. O' CONNOR,*[,2,3] NANCY J. STEVENS,[2,3] and ERIC M. ROBERTS[4]
[1]Department of Biological Sciences, 107 Irvine Hall, Ohio University, Athens, Ohio 45701, U.S.A., eg377304@ohio.edu;
[2]Ohio Center for Ecology and Evolutionary Studies, Irvine Hall, Athens, Ohio 45701, U.S.A.;
[3]Department of Biomedical Sciences, 228 Irvine Hall, Ohio University Heritage College of Osteopathic Medicine, Athens, Ohio 45701, U.S.A., oconnorp@ohio.edu, stevensn@ohio.edu;
[4]School of Earth and Environmental Sciences, James Cook University, Townsville, Queensland 4811, Australia, eric.roberts@jcu.edu.au

ABSTRACT—Whereas titanosaurians represent the most diverse and cosmopolitan clade of Cretaceous sauropod dinosaurs, they remain rare components of Cretaceous African faunas. Currently recognized continental African titanosaurians include *Aegyptosaurus baharijensis* and *Paralititan stromeri* from early Upper Cretaceous deposits near Bahariya Oasis, Egypt, and *Malawisaurus dixeyi* and *Karongasaurus gittelmani* from the Lower Cretaceous (~Aptian) Dinosaur Beds of Malawi, in addition to several undesignated and fragmentary forms across the continent. Here, we describe a new titanosaurian taxon, *Rukwatitan bisepultus*, on the basis of a partial, semiarticulated postcranial skeleton recovered from the middle Cretaceous Galula Formation in southwestern Tanzania. Unique to *Rukwatitan* are carotid processes on posterior cervical vertebrae, a deep coracobrachialis fossa and subquadrangular cross-section of the humerus, and a slender, curved, teardrop-shaped pubic peduncle on the ilium. Parsimony and Bayesian phylogenetic analyses of 35 sauropod taxa congruently place *Rukwatitan* as a non-lithostrotian titanosaurian, a relationship supported by cervical vertebrae with undivided pleurocoels and strongly procoelous anterior caudal vertebrae. *Rukwatitan* differs from the potentially penecontemporaneous and geographically proximate *Malawisaurus* by exhibiting weakly developed chevron articulations and posteriorly inclined neural spines on the middle caudal vertebrae, a proximally robust and distally unexpanded humerus, and an anteroventrally elongated coracoid. Similar to biogeographic patterns identified in certain crocodyliform clades (e.g., small-bodied notosuchians), titanosaurians on continental Africa appear to exhibit a regional (e.g., southern versus northern Africa), rather than a continental- or supercontinental-level signal.

SUPPLEMENTAL DATA—Supplemental materials are available for this article for free at www.tandfonline.com/UJVP

INTRODUCTION

Following the end of the Jurassic Period, titanosauriform sauropods achieved peak diversity and a global distribution by the end of the Cretaceous (Wilson, 2002; Upchurch et al., 2004; Barrett and Upchurch, 2005; Curry Rogers, 2005; Upchurch and Barrett, 2005; Cerda et al., 2012b). Specifically within the titanosauriforms, the diversification of titanosaurians during the Cretaceous coincides with the decline of Diplodocoidea. This latter group diminished in diversity and was restricted to Africa, South America, and Europe through the early Late Cretaceous (Salgado and Bonaparte, 1991; Sereno, 1999; Barrett and Upchurch, 2005; Rauhut et al., 2005; Upchurch and Barrett, 2005; Wilson, 2005; Sereno et al., 2007; Whitlock, 2011). The vast majority of known Cretaceous sauropods pertain to titanosaurians, with South America yielding the majority of named taxa (approximately 39 valid titanosauriform sauropods, many considered titanosaurians; Mannion and Otero, 2012) and providing the best documentation of the diversity present within the clade (Salgado et al., 1997; Leanza et al., 2004; Apesteguía, 2007; Salgado and Bonaparte, 2007; Novas, 2009; Mannion and Calvo, 2011; D'Emic, 2012; Mannion et al., 2013). Recent discoveries in Asia are also expanding our knowledge of titanosaurian diversity (Wilson and Upchurch, 2009; Mannion, 2011; Mannion and Calvo, 2011; D'Emic, 2012). Numerous stem, basal, and derived titanosaurians are recovered from the middle Cretaceous (Aptian–Cenomanian) deposits of South America (e.g., *Andesaurus delgadoi* Calvo and Bonaparte, 1991 [Mannion and Calvo, 2011]; *Argentinasaurus huinculensis* Bonaparte and Coria, 1993; *Chubutisaurus insignis* del Corro, 1975 [Carballido et al., 2011]; *Epachthosaurus sciuttoi* Powell, 1990 [Martínez et al., 2004]; *Ligabuesaurus leanzai* Bonaparte, Gonzalez Riga, and Apesteguía, 2006; *Tapuiasaurus macedoi* Zaher, Pol, Carvalho, Nascimento, Riccomini, Larson, Juárez-Valieri, Pires-Domingues, da Silva, and de Almeida Campos, 2011; for a more inclusive list, see Mannion and Calvo, 2011:table 7), yet members of the clade remain rare components in contemporaneous Cretaceous terrestrial faunas of Africa. Four titanosaurians have been formally recognized from Cretaceous deposits on continental Africa: *Karongasaurus gittelmani* and *Malawisaurus dixeyi* (Jacobs et al., 1993; Gomani, 2005) from the Aptian Dinosaur Beds (DB) of Malawi and *Paralititan stromeri* and *Aegyptosaurus baharijensis* (Stromer, 1932; Smith et al., 2001) from the Cenomanian Bahariya Formation of Egypt. *Karongasaurus* is based on an isolated dentary and several referred cylindrical teeth with

*Corresponding author.
Color versions of one or more figures in this article can be found online at www.tandfonline.com/ujvp.

high-angled wear facets, with the latter traits considered derived titanosaurian features (Wilson, 2002; Gomani, 2005; Zaher et al., 2011). *Malawisaurus* is based on several associated partial skeletons and a variety of referred isolated cranial and postcranial elements that represents the most complete African titanosaurian (collected from seven different localities; Gomani, 2005:table 1). *Paralititan* is based on an associated postcranial skeleton of an extremely large individual (Smith et al., 2001), and *Aegyptosaurus baharijensis* (Stromer, 1932) has been considered a titanosaurian (Upchurch, 1995; Wilson, 2002; Upchurch et al., 2004) or titanosauriform (Wilson and Sereno, 1998). Unfortunately, specimens of *Aegyptosaurus* were destroyed during World War II (Smith et al., 2001). *Angolatitan adamastor* (Mateus et al., 2011), from the late Turonian Tadi Beds of Angola, has been recovered as a titanosauriform (Mateus et al., 2011; some topologies of Mannion et al., 2013) or a potential titanosaurian (D'Emic, 2012; some topologies of Mannion et al., 2013) and is based on a partial right forelimb. Additional titanosaurian material has been recovered from continental Africa but is generally too fragmentary to properly assign to lower taxonomic levels (Greigert et al., 1954; Lapparent, 1960; Broin et al., 1974; Kennedy et al., 1987; Bellion et al., 1990; Moody and Sutcliffe, 1990; Sereno et al., 1999; O'Leary et al., 2004; O'Connor et al., 2006; D'Emic and Wilson, 2012).

Hence, the discovery of a novel titanosaurian provides important new information on middle Cretaceous faunas from continental Africa and will help differentiate faunal elements recovered from the Rukwa Rift Basin of southwestern Tanzania from potentially penecontemporaneous faunas from other parts of the continent (e.g., the Dinosaur Beds of Malawi, various circum-Saharan locales). Here, we describe a new titanosaurian, *Rukwatitan bisepultus*, consisting of a partial, associated postcranial skeleton from the middle Cretaceous Galula Formation (Aptian–Cenomanian) of southwestern Tanzania (Figs. 1–2). This discovery sheds light on the early evolutionary history of titanosaurians outside of South America and prior to their Late Cretaceous dominance. The new African titanosaurian further expands upon existing phylogenetic, paleobiological, and regional paleobiogeographical perspectives for sauropods specifically and Gondwanan terrestrial vertebrate faunas more generally (Sereno et al., 2004; Curry Rogers, 2005; Krause et al., 2006, 2007; O'Connor et al., 2006; Sereno and Brusatte, 2008; Wilson and Upchurch, 2009; D'Emic, 2012).

TABLE 1. Selected measurements (in mm) of *Rukwatitan bisepultus*.

Element	CL	ACH	ACW	PCH	PCW	NASH
APCV	492	100	174	106	195	—
PCV	478	—	—	—	—	—
UCV	—	—	—	—	—	—
Dvna1	—	—	—	—	—	—
ACV (A)	104	169	151	151	134	182
ACV (B)	—	141	—	144	—	—
ACV (C)	107	—	—	129	149	—
MCV (1/3)	113	128	132	—	—	153
MCV (2/3)	116	—	—	—	—	145
MCV (3/3)	121	—	—	122	114	132
MCV (A)	120	115	126	113	122	—
MCV (B)	131	108	104	107	97	110
MCV (C)	107	79	—	75	—	—
	L	PW	MW	DW		
Scapula blade	620	193	155	284		
Humerus (H)	910	321	136	260		
Humerus (R)	1015	297	114	—		

Vertebral elements are listed in anterior-posterior order. Dashes indicate where measurements could not be taken because of damage, missing, or inaccessible areas. **Abbreviations**: **ACH**, anterior centrum height; **ACV**, anterior caudal vertebra; **ACW**, anterior centrum width; **APCV**, antepenultimate cervical vertebra; **CL**, centrum length (excluding condyles); **DVna1**, neural arch of first dorsal vertebra; **DW**, distal width; **H**, holotype; **L**, element length; **MCV**, middle caudal vertebra; **MW**, midlength width; **NASH**, neural arch and spine height; **PCH**, posterior centrum height; **PCV**, penultimate cervical vertebra; **PCW**, posterior centrum width; **PW**, proximal width; **R**, referred; **UCV**, ultimate cervical vertebra.

MATERIALS AND METHODS

Computed Tomography—Materials of *Rukwatitan bisepultus* (RRBP 07409) were scanned on a Philips Brilliance computed tomography (CT) 64-channel scanner using the following protocol: 120 kV, 200 mA, and a slice thickness of 1.0 mm. Digital visualization of raw DICOM files was completed in Avizo 6.3 (Visualization Science Group (VSG)/FEI, U.S.A.).

Institutional Abbreviations—**MAL**, Malawi Department of Antiquities, Lilongwe, Malawi; **RRBP**, Rukwa Rift Basin Project, Tanzanian Antiquities Unit, Dar es Salaam, Tanzania; **TNM**, Tanzanian National Museums, Dar es Salaam, Tanzania.

SYSTEMATIC PALEONTOLOGY

DINOSAURIA Owen, 1842
SAURISCHIA Seeley, 1887
SAUROPODA Marsh, 1878
TITANOSAURIA Bonaparte and Coria, 1993
RUKWATITAN BISEPULTUS, gen. et sp. nov.
(Figs. 3–12)

Etymology—*Rukwatitan*, from 'Rukwa' (masc.), referring to Lake Rukwa of southwestern Tanzania and the structural rift basin of the same name from which the holotype and referred humerus were recovered, and 'titan' (Greek), offspring of Uranus and Gaea, symbolic of brute strength and large size; *bisepultus* (Latin), twice buried, in reference to dual nature of holotype specimen being initially entombed in an overbank-derived mudstone, with a portion of the same skeleton later being mobilized by a paleochannel and reburied nearby as part of a channel sandstone facies.

Holotype—Rukwa Rift Basin Project (RRBP) 07409, partial skeleton including three posterior cervical vertebrae, one partial anterior dorsal vertebral neural arch, three anterior caudal vertebrae, six middle caudal vertebrae, two chevrons, multiple partial dorsal ribs, distal left scapula, partial left and right coracoids, left humerus, partial right ulna, left ilium, and proximal right pubis (Fig. 3). Discovered by J. J. W. Sertich on June 9, 2007.

Type Locality and Horizon—Locality RRBP 2007-02 (Namba 2), approximately 25 km south of Lake Rukwa in the Galula Study Area, in the middle portion of the Namba Member, Galula Formation, Rukwa Rift Basin, southwestern Tanzania (locality coordinates on file at Ohio University and with the Tanzania Antiquities Unit). The only other fossil yet identified from the Namba 2 locality is a partial peirosaurid crocodyliform *Rukwasuchus yajabalijekundu* (Sertich and O'Connor, 2014).

Localities and Referred Specimens—RRBP 03151, right humerus (Fig. 10H–K) referred to *Rukwatitan bisepultus*, was recovered from locality RRBP 2003-10.

Age and Distribution—Materials described herein were recovered from the middle portion of the Namba Member of the Galula Formation of the Red Sandstone Group, Rukwa Rift Basin, southwestern Tanzania (Fig. 1). Based on several lines of geological and faunal evidence, the age of the Galula Formation has been constrained to the middle Cretaceous (Aptian–Cenomanian), with best estimates between 100 and 110 Ma (Roberts et al., 2004, 2010, 2012; O'Connor et al., 2006, 2010). The Namba Member (Fig. 2) is dominated by very fine- to medium-grained sandstones, with minor mudstone and siltstone lenses representing deposition within a broad fluvial braidplain system (Roberts et al., 2010).

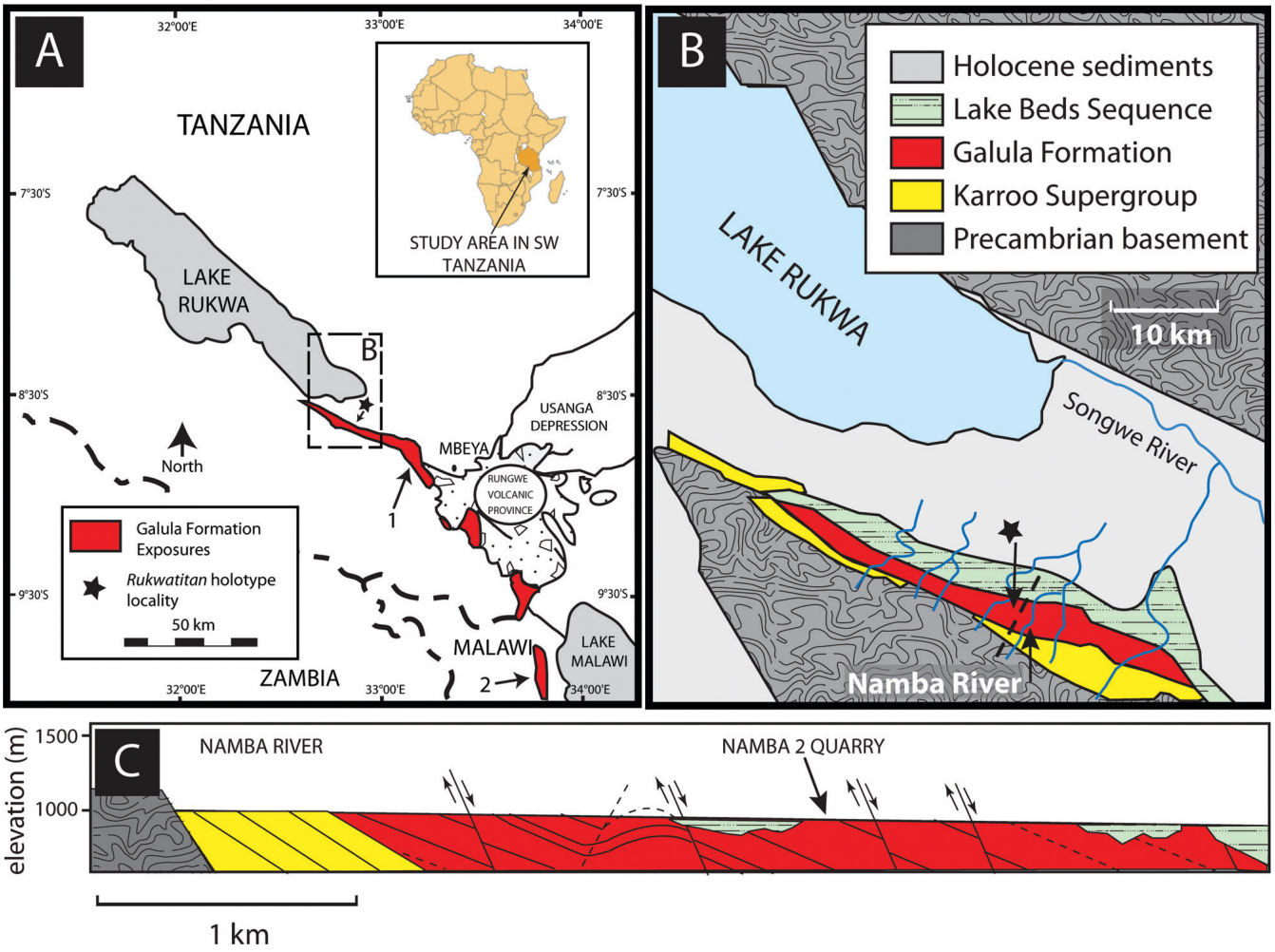

FIGURE 1. Expanded (**A**) and detailed (**B**) regional maps to illustrate exposures of the middle Cretaceous Galula Formation (red/dark gray) in southwest Tanzania. The location of the type locality (RRBP 2007-02; Namba 2) of *Rukwatitan bisepultus* is denoted by black stars in **A** and **B**, with locality TZ-10 indicated by the '1' in **A**. The location of the Malawi Dinosaur Beds is denoted by '2' in **A** and is shown to illustrate the proximity of the two units relative to one another. **C**, basin cross-section approximating the hashed line in **B**, showing the stratigraphic and structural relationships among the dinosaur-bearing Galula Formation, the underlying Karoo Supergroup, and the overlying Lake Beds sequences. The approximate location of the Namba 2 locality in **C** is denoted by the large, single-headed black arrow. Opposing arrows bracketing thin lines illustrate fault structures through the cross-section.

Diagnosis—Titanosaurian sauropod diagnosed by the following suite of autapomorphies: ventral surface of posterior cervical vertebrae with (1) weakly developed carotid processes posteriorly and (2) paired shallow fossae anteriorly that are not separated by a thin keel; (3) posterior cervical vertebrae with anteroposteriorly elongate and undivided fossa posterior to the anterior centrodiapophyseal lamina that deeply invades the ventral surface of the diapophysis; (4) accessory tubercle on the ventral surface of the cervical rib capitulum, lateral to the capituloparapophyseal suture; (5) deep coracobrachialis fossa on proximal humerus bounded by strong anteriorly projecting deltopectoral crest and strong anteromedial ridge, extending to approximately the humeral midshaft; (6) flattened anterior, medial, lateral, and posterior surfaces at the humeral midshaft, resulting in a subquadrangular cross-section; and (7) pubic peduncle on the ilium that is teardrop-shaped, with the 'tail' curving posteriorly, slightly longer transversely than anteroposteriorly.

Additionally, the following combination of phylogenetically informative characters assist with the placement of *Rukwatitan bisepultus* as a basal titanosaurian: undivided pleurocoels on cervical vertebrae; strongly procoelous anterior caudal vertebrae, with the apex of the posterior condyle positioned on the dorsal half of the centrum; pedicles of the neural arch attached to the anterior half of caudal vertebral centrum; unforked chevrons with a deep hemal canal; and squared proximolateral corner of the humerus. Notably, *Rukwatitan* lacks the ventral longitudinal hollow on the caudal vertebral series typical of many other titanosaurians.

SEDIMENTOLOGIC AND TAPHONOMIC CONTEXT

Whereas the vast majority of fossil localities in the Galula Formation represent isolated elements, a handful of associated to near-perfectly articulated skeletons and rare bonebeds do exist. With two exceptions, all of the multielement bone accumulations and most of the isolated bones collected during the course of 11 field seasons in the Cretaceous succession are all preserved within fluvial channel sandstones. The titanosaurian specimen recovered from locality RRBP 2007-02 (Namba 2) represents

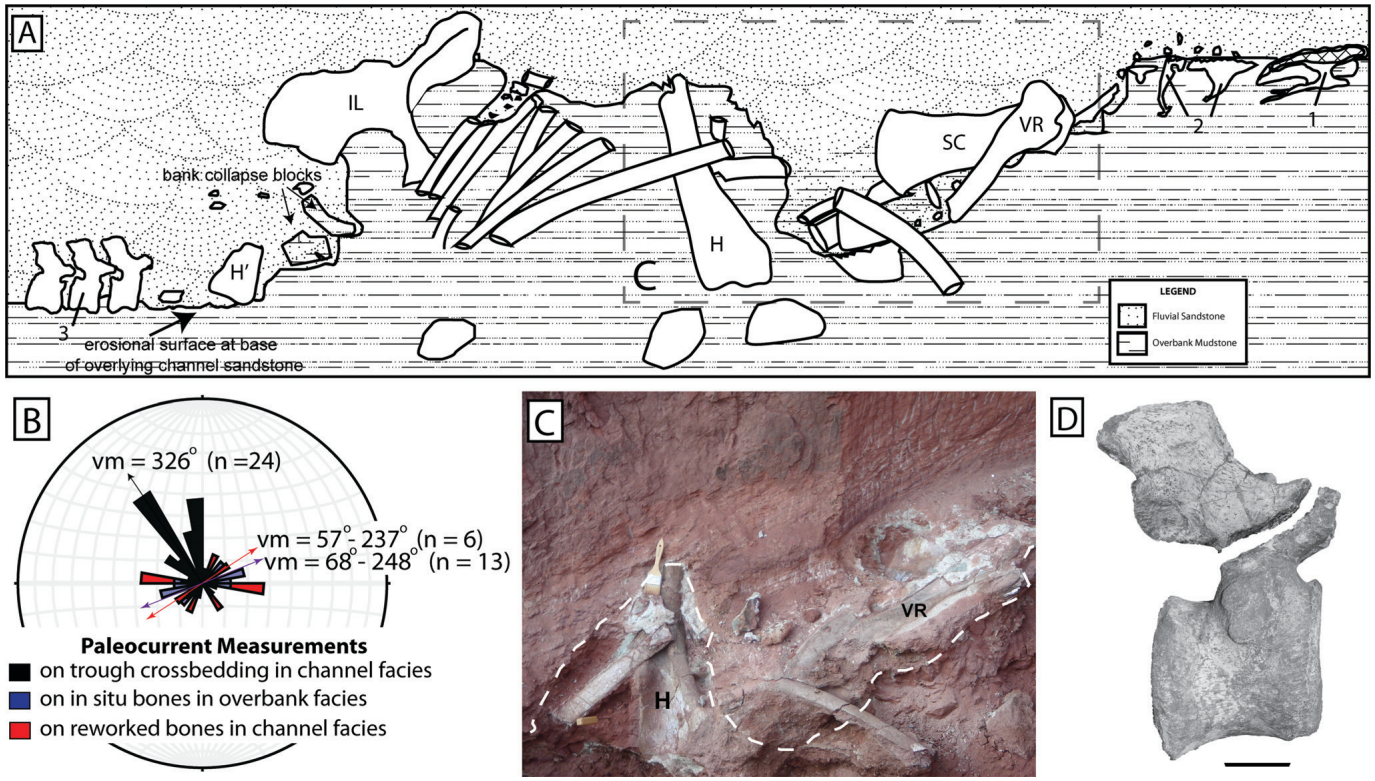

FIGURE 2. Quarry map (**A**) of locality Namba 2 and rose diagram (**B**) to indicate predominant paleocurrent orientations of elements in different facies; **C**, photograph of in situ skeletal elements of *Rukwatitan bisepultus* (RRBP 07409) in the quarry wall at locality RRBP 2007-02 (Namba 2) to illustrate the distinction between overbank and channel facies (see white hashed line); **D**, middle caudal vertebra of *Rukwatitan bisepultus* in left lateral view illustrating matching contact areas of a single bone that was partially eroded (in the deep past), mobilized over a very short distance (approximately 1.5 m), and redeposited as part of a channel facies. **Abbreviations**: **H**, left humerus, proximal portion; **H'**, left humerus, distal portion; **IL**, left ilium; **SC**, left scapular blade; **VR**, vertebral rib; **1**, map view of antepenultimate cervical vertebra (Fig. 4A–F); **2**, map view of longitudinally sectioned vertebral series (PCV, UCV, DVna1; as anatomically illustrated in Fig. 4G); **3**, map view of articulated middle caudal series (Fig. 7A–C). Scale bar in **D** equals 5 cm.

one of the most remarkable vertebrate fossil accumulations in the Galula Formation. It reveals a window into the genesis of the archetypical channel-hosted vertebrate fossil accumulations in the Galula Formation, and indeed more generally. The *Rukwatitan bisepultus* holotype material can confidently be assigned to a single individual, although paradoxically, the partially articulated skeleton is preserved both as an autochthonous overbank assemblage and allochthonous fluvial channel assemblage. The site preserves a partially articulated skeleton entombed within a fine-grained overbank mudstone that was subsequently incised into and partially eroded and transported by a high-energy fluvial channel (Fig. 2A, B). The fluvial system transported many of the smaller elements away; however, the channel belt rapidly filled back in and much of the eroded skeleton was transported only a few meters and redeposited within the base of the channel sandstone facies.

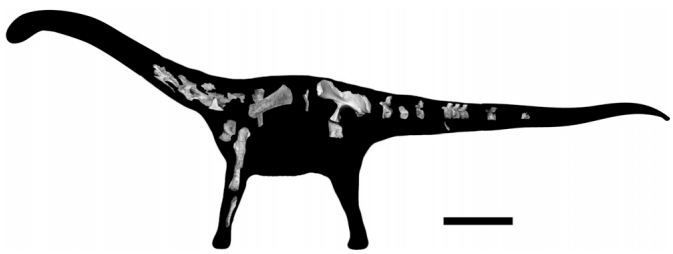

FIGURE 3. Silhouette reconstruction of *Rukwatitan bisepultus* to illustrate those portions of the skeleton recovered from locality RRBP 2007-02 and included as part of the holotype. Scale bar equals 1 m.

The site was discovered in a steep alcove oriented perpendicular to the Namba River bed, providing a three-dimensional (3-D) cross-sectional view of the bones and their relationship with the entombing strata. A traditional quarry with a plane view orientation and excavation strategy was not possible due to the steep, cliff-like nature of the exposure. Instead, the excavation proceeded from the alcove wall inwards, resulting in a cross-sectional style quarry map (Fig. 2A). Irrefutable evidence of the association between allochthonous channel elements and the autochthonous overbank elements comes in the form of multiple precisely matched broken elements between the two facies that yield perfect jigsaw-like fits along matching broken ends of bones (e.g., a caudal vertebra, Fig. 2D; left humerus, Fig. 10A–D). The in situ overbank-hosted skeleton includes a string of partially articulated cervical vertebrae and dorsal ribs, along with associated portions of the pelvic and pectoral girdles and forelimb elements. Other than the partial right ulna and partial right pubis, both of which were recovered from the channel facies, all other elements are derived from the left side of the animal and were recovered in the overbank facies. Moreover, the articulated cervical vertebral series preferentially preserve the lower left side of the elements. Whereas the dorsal aspect of the neural arches was eroded by the paleochannel, the right side of the vertebral

series was eroded immediately prior to discovery and excavation. The fluvial assemblage of bones from this skeleton is dominantly composed of large, robust elements, although abundant bone fragments also exist. Presumably, some of the lighter material was transported downstream. Large mudstone bank collapse blocks are also directly associated with the bones within the base of the incised channel, demonstrating that the channel rapidly filled after down-cutting into the overbank mudstone-hosted skeleton. Unfortunately, the site was discovered in a relatively freshly eroded alcove along the banks of the Namba River, suggesting that a significant portion of the otherwise articulated/associated skeleton was likely lost to modern erosion. This makes it difficult to fully assess how much of the skeleton was present, prior to the fluvial incision and entrainment of the bones into the channel sandstone facies.

DESCRIPTION

Cervical Vertebrae

Two posterior cervicals, one 'cervicodorsal,' and a portion of the succeeding dorsal neural arch were recovered in articulation from the Namba 2 quarry. Hence, the recovered presacral vertebral series of *Rukwatitan bisepultus* spans the cervicodorsal transition. For consistency within this contribution and because the exact regional vertebral count in *Rukwatitan* is not known, the recovered vertebrae will be discussed as follows: the first preserved vertebra of the series will be designated as APCV (antepenultimate cervical vertebra); the second preserved vertebra of the series will be designated at PCV (penultimate cervical vertebra); the third preserved vertebra of the series will be designated as UCV (ultimate cervical vertebra); and the final fragmentary neural arch of the series will be designated as DVna1 (neural arch of the first dorsal vertebra).

The first two cervical vertebrae in the series (APCV and PCV) have fused cervical ribs, with the succeeding vertebra (UCV) exhibiting a fused bony loop that lacks the extended body of the rib (Fig. 4A, E–G). The next element in the series (DVna1) exhibits the unfused condition, with a distinct articulation present at the diapophyseal articular surface (Fig. 4G). Interpretation of the dorsal neural arch fragment is based on the presence of a preserved diapophysis that is in articulation (but not fused) with the tuberculum of a partial dorsal rib and marked increase in length of the centroprezygapophyseal lamina. Whereas cervical ribs and cervical vertebrae typically fuse during ontogeny, dorsal ribs do not normally fuse with their respective dorsal vertebrae.

All three cervical vertebrae preserve at least some components of the centrum and the neural arch. The first two vertebrae of the series (Fig. 4A–G) are the most complete and provide information regarding the centrum and ventral portion (e.g., pedicles, zygapophyses) of the neural arch, whereas the two posterior vertebrae are fairly incomplete. The dorsal portion of each neural arch (e.g., neural spines, laminae) is not preserved due to post-depositional Cretaceous-age channel incision, erosion, and reburial of part of the skeleton. A clear erosional scour surface is evident within the quarry and along the dorsal portion of the vertebral series and the ilium (Fig. 2A). The right half of PCV and UCV and most of DV1 were lost to modern erosion and represent the state of the materials at the time of discovery. Exposed along the erosional surfaces within all of the recovered presacral vertebrae is the internal camellate tissue structure typical of somphospondylian titanosauriforms (Wilson and Sereno, 1998; D'Emic, 2012).

Regarding the more complete vertebra (APCV), the centrum is dorsoventrally compressed, imparting a low and wide profile (Fig. 4C, E). The prezygapophysis is low and positioned immediately dorsal to the dorsal limit of the centrum, with the interprezygapophyseal distance approximately twice the width of the condyle (Fig. 4C). The distance between the prezygapophyses is comparable to that in posterior cervical vertebrae of other titanosaurians such as *Rapetosaurus krausei* (Curry Rogers, 2009:fig. 12), but is noticeably wider and closer to the centrum than the prezygopophyses of the posterior vertebrae in *Trigonosaurus pricei* (Campos et al., 2005:fig. 3). The preserved relatively high-angled spinoprezygapophyseal and postzygodiapophyseal lamina (Fig. 4F) suggest that the neural spine of the vertebra would have been quite tall as expected in this vertebral transition zone.

Vertebral centra of APCV and PCV are well preserved and strongly opisthocoelous, exhibiting a ventral margin of the posterior cotyle that extends further posteriorly than the dorsal margin (Fig. 4E, G). The centrum is elongate and dorsoventrally compressed in APCV and PCV, but is considerably anteroposteriorly shorter in the UCV (see Table 1 for metrics; Fig. 4). A large, oval, undivided pleurocoel is present on the lateral surface of the centrum in both APCV and PCV, as in many titanosaurians (Wilson, 2002). The deepest portion of the pleurocoel occurs at the level of the parapophysis and shallows considerably towards both the anterior and posterior ends of the centrum. The dorsal surface of the parapophysis is not excavated. A pneumatic fossa is located anterior to the rather small and short anterior centrodiapophyseal lamina (ACDL). Posterior to the ACDL is an anteroposteriorly elongate fossa that invades the diapophysis dorsally from the pleurocoel such that a thin layer of the diapophysis and part of the posterior centrodiapophyseal lamina separates this fossa from the infrapostzygapophyseal fossa (postzygapophyseal centrodiapophyseal fossa; Wilson et al., 2011) of the neural arch (PCV in Fig. 4G; APCV in Fig. 5B). This relatively deep, undivided, and elongate fossa represents a potential autapomorphy until better material is recovered and additional studies of titanosaurian pleurocoel morphologies are completed. The ventral surface of the centrum is slightly concave longitudinally and moderately concave laterally, such that the parapophysis projects just ventrolaterally from the anterior half of the centrum (Fig. 4B, E–G). The ventral surface of the centrum (at least in APCV) also exhibits (1) paired shallow subcircular fossae immediately lateral to the midline at the level of the parapophysis but without a sharply defined keel; and (2) low bilateral ridges set just off of the midline that run along the anteroposterior axis (Fig. 5A, C, E). The paired ventral fossae may be similar to the concavities described in fragmentary cervical vertebrae of uncertain position in the titanosaurian *Gondwanatitan faustoi* and the first three cervical vertebrae of *Mongolosaurus haplodon*; however, the concavities are deeper, and elongated along the midline axis on the former and are separated by a prominent bony ridge or keel in both taxa (Kellner and Azevedo, 1999:fig. 5; Mannion, 2011:fig. 8). The ridges (tentatively referred to as carotid processes in this study and previously reported to not be present in sauropods; Wedel and Sanders, 2002) are best developed in APCV and only incipiently present in PCV. The carotid process, at least in Aves, serves as the origin for the flexor colli medialis and ventrails muscles and bound the carotid fossa (Baumel and Witmer, 1993; Wedel and Sanders, 2002). Together, these two features of the ventral surface of the posterior cervical vertebrae are considered autapomorphies of *Rukwatitan.* At the point of fusion between the parapophysis and the costal capitulum, a small process projects posteriorly from the robust suture that characterizes the fused capituloparapophyseal ramus (Fig. 5D). A tubercle is present on the ventral surface of the capitulum just lateral to this suture on both the APCV and PCV (Fig. 5A, D). The tubercle may represent a region of remodeled bone marking the line of fusion at the capituloparapophyseal suture. Until this is better characterized among sauropods more generally, it remains unclear whether this represents transient morphology related to the precise ontogenetic stage of this individual or a taxon-specific characteristic. This tubercle is absent from posterior cervical

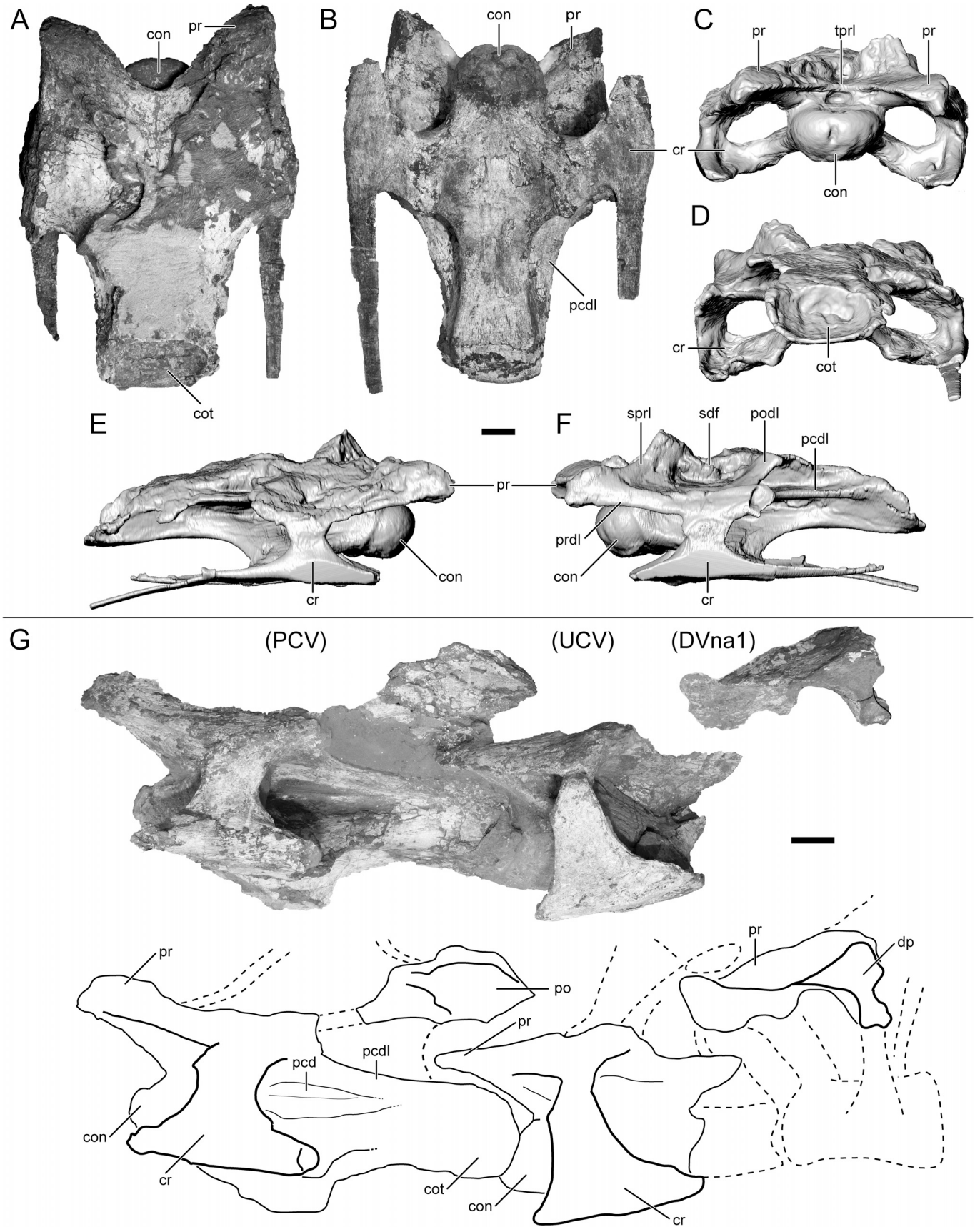
A
con
pr
cot
B
con
pr
pcdl
C
pr
tprl
pr
cr
con
D
cr
cot
E
pr
con
cr
F
sprl
sdf
podl
pcdl
prdl
con
cr
G
(PCV)
(UCV)
(DVna1)
pr
po
pr
pcd
pcdl
con
cr
cot
con
cr
pr
dp

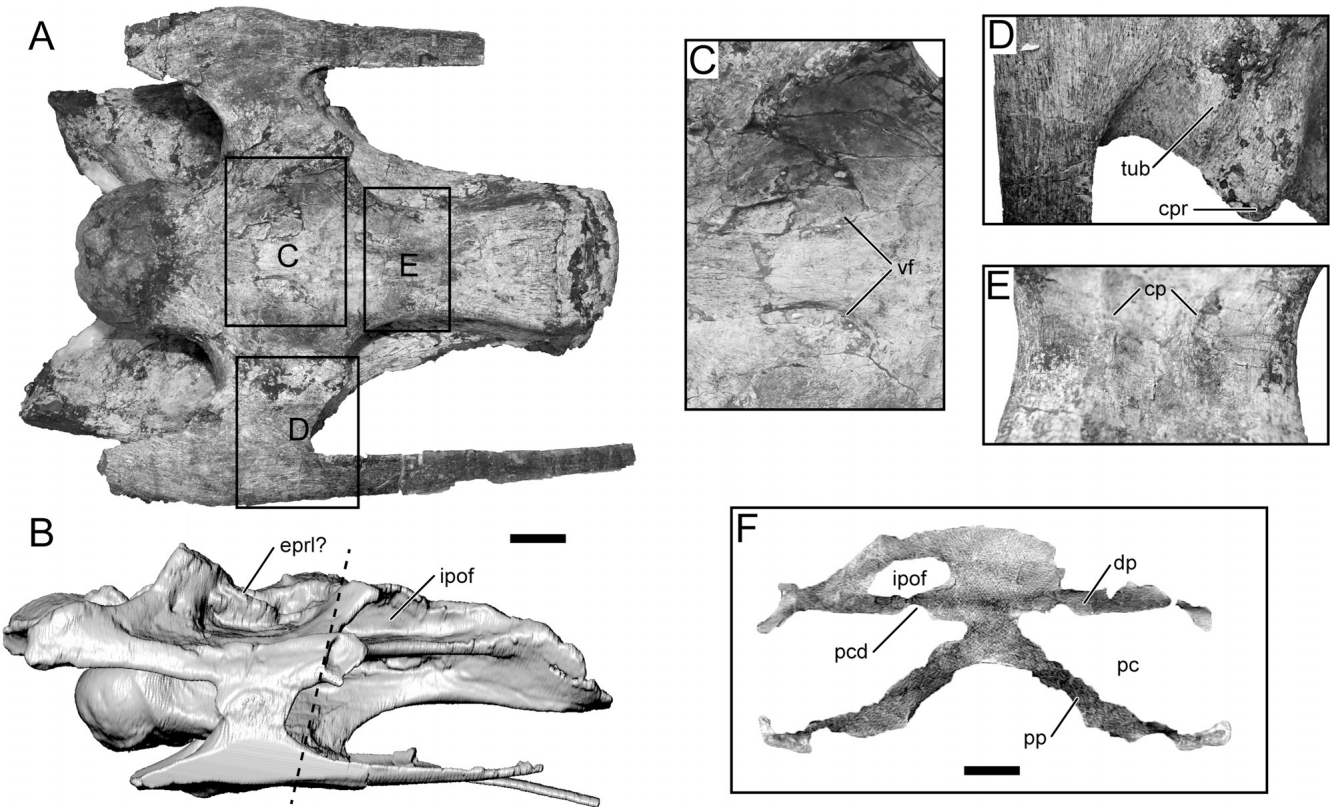

FIGURE 5. Posterior cervical vertebra of *Rukwatitan bisepultus* (RRBP 07409; APCV in Description). **A**, ventral; **B**, left lateral views showcasing key features. **B** is a digital reconstruction based on computed tomography (CT) scans. Insets **C** and **D** are in close ventral views. Inset **E** is in postero-ventral view. Anterior is to the left in both **A** and **B**. Insets **D** and **E** are rotated 90° clockwise relative to **A**. Dashed line in **B** represents where the transverse cross-section of **F** was taken from the CT scans. **Abbreviations**: **cp**, carotid processes; **cpr**, capituloparapophyseal ramus; **dp**, diapophysis; **eprl?**, epipophyseal-prezygapophyseal lamina?; **ipof**, infrapostzygapophyseal fossa; **pc**, pleurocoel; **pcd**, pleurocoel, dorsal expansion; **pp**, parapophysis; **tub**, tubercle; **vf**, ventral fossa. Scale bar equals 5 cm in **A**, **B**, and **F**.

vertebrae of the basal titanosaurian *Malawisaurus dixeyi* (Gomani, 2005) and derived titanosaurians *Trigonosaurus pricei* (Campos et al., 2005:figs. 10, 14) and *Rapetosaurus krausei* (Curry Rogers, 2009) and is provisionally considered an autapomorphy of *Rukwatitan.* The centroprezygapophyseal lamina is short and undivided, with a small fossa present medially on the lamina and ventral to the intraprezygapophyseal lamina (Fig. 4C). The posterior centrodiapophyseal lamina is long and curves medially along its course. The bases of the left spinoprezygapophyseal and postzygadiapophyseal laminae are preserved on the centrum of APCV (Fig. 4F). The spinoprezygapophyseal lamina is angled steeply posteromedially, with the postzygadiapophyseal lamina angled only moderately in a posteromedial direction. The spinodiapophyseal fossa, bounded by the neural spine, prezygapophysis, postzygapophysis, and diapophysis, is deep and may have a weakly developed subhorizontal lamina (epipophyseal-prezygapophyseal lamina, EPRL; Wilson and Upchurch, 2009; Wilson et al., 2011; Wilson, 2012) that divides the fossa into dorsal and ventral portions (Fig. 5B). The EPRL is present in several neosauropods and some theropods that exhibit a prominent epipophysis (Wilson, 2012). The thin and fragmentary nature of the lamina precludes any unequivocal assessment in *Rukwatitan*, but the preserved morphology is at least suggestive that it was present.

Caudal Vertebrae

Three anterior caudal vertebrae were recovered. Although two vertebrae are incomplete, both missing various portions of the centrum and the neural arch (Fig. 6G–L), the other specimen is well preserved and missing only the right prezygapophyseal facet and the tip of the neural spine (Fig. 6A–F). The two anterior-most caudal vertebrae (Fig. 6A–I) have a centrum that is strongly procoelous, a trait that is typical of most titanosaurians (Salgado et al., 1997; Sanz et al., 1999; Wilson, 2002, 2006; see Phylogenetic Relationships, below). The posteriorly projecting condyle is asymmetrically skewed dorsally in the anterior-most caudal vertebra. The other anterior caudal vertebra (Fig. 6J–L) is amphiplatyan-amphicoelous and suggests that the strongly procoelous condition in *Rukwatitan* is only present within the most proximal caudal vertebrae. A similar pattern of the

← FIGURE 4. Posterior cervical vertebra and cervicodorsal vertebral series of *Rukwatitan bisepultus* (RRBP 07409). **A**–**F**, posterior cervical vertebra (APCV in description); **A**, dorsal; **B**, ventral; **C**, anterior; **D**, posterior; **E**, right lateral; and **F**, left lateral views. **C**–**F** are digital reconstructions based on computed tomography (CT) scans. **G**, cervicodorsal series in left lateral view with interpreted outline below. **Abbreviations**: **con**, condyle; **cot**, cotyle; **cr**, cervical rib; **dp**, diapophysis; **DVna1**, first neural arch of dorsal vertebra; **pcd**, pleurocoel, dorsal expansion; **pcdl**, posterior centrodiapophyseal lamina; **PCV**, penultimate cervical vertebra; **po**, postzygapophysis; **podl**, postzygodiapophyseal lamina; **pr**, prezygapophysis; **prdl**, prezygodiapophyseal lamina; **sdf**, spinodiapophyseal fossa; **sprl**, spinoprezygapophyseal lamina; **tprl**, intraprezygapophyseal lamina; **UCV**, ultimate cervical vertebra. Scale bar equals 5 cm.

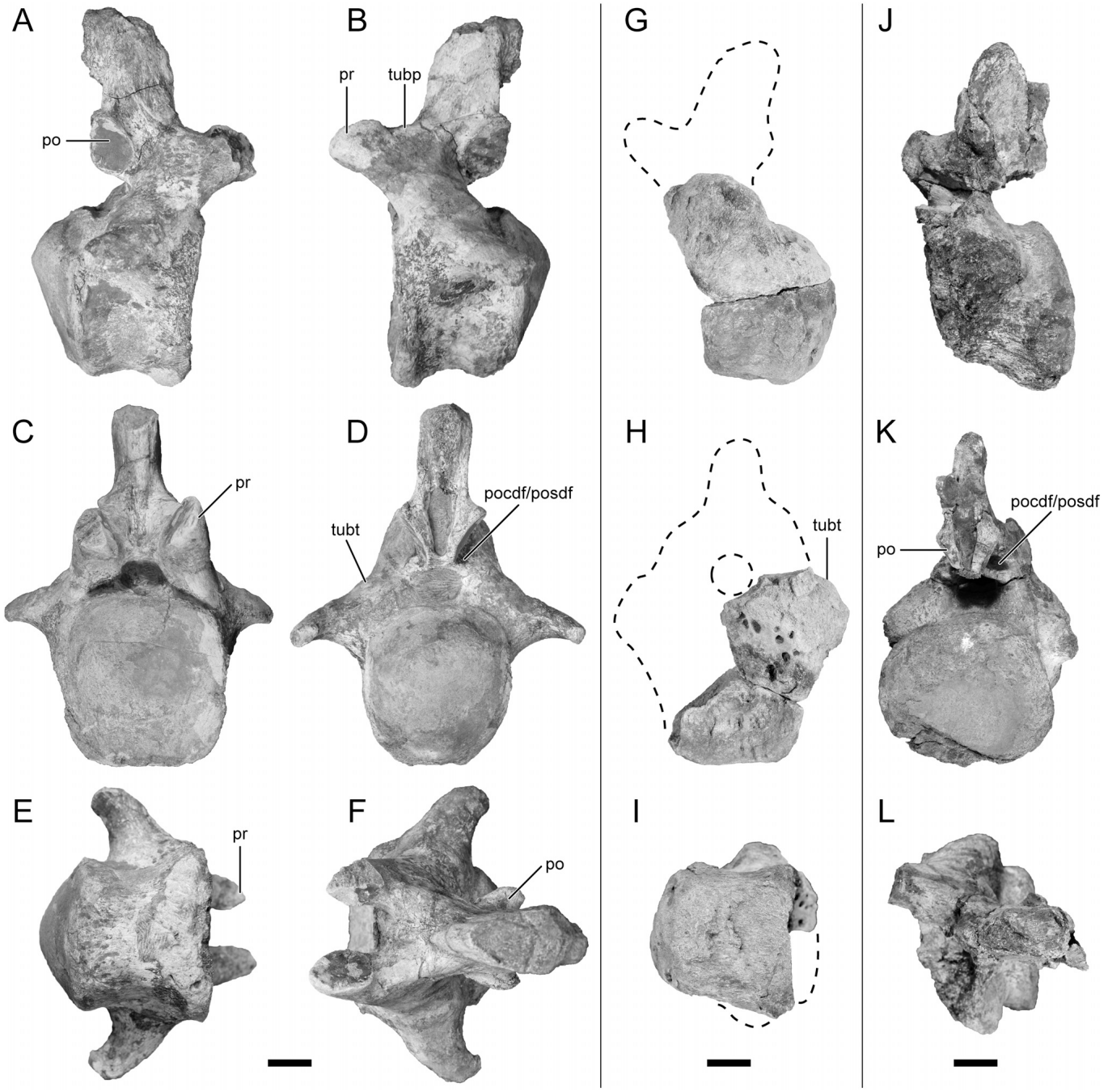

FIGURE 6. Anterior caudal vertebrae of *Rukwatitan bisepultus* (RRBP 07409). **A**–**F**, proximal-most anterior caudal vertebra; **A**, right lateral; **B**, left lateral; **C**, anterior; **D**, posterior; **E**, ventral; and **F**, dorsal views. **G**–**I**, second recovered anterior caudal vertebra; **G**, left lateral; **H**, anterior; and **I**, ventral views. **J**–**L**, third recovered anterior caudal vertebra; **J**, left lateral; **K**, posterior; and **L**, dorsal views. Anterior is to the left in **B**, **F**, **G**, and **J** and to the right in **A**, **E**, and **I**. **Abbreviations**: **po**, postzygapophysis; **pocdf/posdf**, postzygapophyseal centrodiapophyseal/spinodiapophyseal fossa; **pr**, prezygapophysis; **tubp**, tubercle of prezygapophysis; **tubt**, tubercle of the transverse process. Scale bars equal 5 cm.

procoelous-to-amphicoelous progression along the caudal vertebral series is exhibited by the basal titanosaurians *Andesaurus delgadoi* (the procoelous condition is only incipient; Calvo and Bonaparte, 1991; Mannion and Calvo, 2011), *Malawisaurus dixeyi* (Gomani, 1999, 2005), and *Traukutitan eocaudata* (Juárez Valieri et al., 2011). The cotyle is subrectangular, being taller than wide, with rounded corners (Fig. 6C). The anteroposterior length of the centrum is short, giving the centrum a tall appearance. The lateral and ventral surfaces of the centrum are slightly concave, flaring peripherally toward the margin of the anterior articulation. Although there is not a significant depression on the lateral surface of the centrum ventral to the transverse process, a few small fossae are present. The overall shape of the centrum is similar to a subrectangular box rather than a cylinder, a condition exhibited by all recovered caudal vertebrae of *Rukwatitan*. The anterior and posterior chevron facets are

reduced, with a slight concavity occupying the space between the right and left sides of each pair. There is no ventrolateral ridge that connects the anterior and posterior chevron facets. A longitudinal ventral hollow on caudal vertebrae, typically considered a titanosaurian character (Wilson, 2002; Curry Rogers, 2005; D'Emic 2012), is not present in *Rukwatitan*. The neural arch is positioned over the anterior half of the centrum, with a transverse process that projects laterally at the dorsal limit of the centrum. The former trait has been used to characterize Titanosauriformes (Upchurch, 1995, 1998; Salgado et al., 1997; Wilson, 2002; Curry Rogers, 2005). The transverse process pinches distally, forming a dorsoventrally restricted, rounded plank that exhibits a slight posterior curve (Fig. 6C, E). This posterior curve extends to the posterior margin of the centrum, similar to the anterior caudal vertebrae of some titanosauriforms such as *Malawisaurus* (Gomani, 2005). This differs from the condition exhibited by *Andesaurus* and other titanosauriforms in which it extends past the posterior margin of the centrum (Mannion and Calvo, 2011; Mannion et al., 2013). A subtle tubercle lies near the junction of the transverse process and the neural arch. This feature is well developed in the more derived titanosaurians such as *Baurutitan britoi* (Kellner et al., 2005) and *Epacthosaurus scuittoi* (Martínez et al., 2004). The neural arch is robust and exhibits a tall neural spine that angles slightly posterodorsally (Fig. 6B, D). Whereas the prespinal and postspinal laminae are present, laminae formed by the confluence of the spinoprezygapophyseal and spinopostzygapopyhseal laminae are only weakly developed. Both prespinal and postspinal fossae are present, with the postspinal fossa being deeper than the prespinal fossa (Fig. 6C, D). Several small fossae line the walls within the prespinal fossa. The prezygapophysis projects anteriorly past the anterior margin of the centrum. A subtle tubercle is present on the spinoprezygopophyseal lamina between the facet and the neural spine. This tubercle extends ventrally along the medial surface as a ridge. This feature is also present in saltasaurids, *Phuwiangosaurus*, and *Tangvayosaurus* (D'Emic, 2012). The prezygapophyseal facet is subcircular and is steeply angled dorsomedially. The intraprezygapophyseal lamina is restricted to a small contribution at the ventral limit of the prespinal fossa (Fig. 6C). There is a weakly excavated postzygapophyseal centrodiapophyseal/spinodiapophyseal fossa (Wilson et al., 2011) just anterior to the postzygapophysis (Fig. 6D, K). The postzygapophyseal facet is directed ventrolaterally, roughly teardrop-shaped, with the tail directed dorsally, and slightly concave. The intrapostzygapophyseal lamina is present and thin.

A total of six middle caudal vertebrae (Figs. 2D, 7), including an articulated series of three vertebrae, were recovered. All are very well preserved except for two specimens. In the first incomplete specimen, the neural arch is sheared along an oblique plane and only preserves the centrum, pedicles, and prezygapophyses. Fortunately, a partial neural arch that includes the neural spine and postzygapophyses was recovered separately from the quarry. The broken edges of each partial vertebra are complementary (e.g., part of the vertebrae was found in the in situ mudstone facies and the other part was found in the adjacent fluvial sandstone facies), thereby allowing a direct association between the two pieces (Fig. 2D; see Sedimentologic and Taphonomic Context, above). The second incomplete specimen is a recovered distal middle caudal and is heavily eroded, preserving a partial and damaged centrum and the base of the neural arch (Fig. 7I–L). The centrum of the anterior-most middle caudal vertebra is slightly rhomboidal in lateral view, canting anteriorly (Fig. 7A). The other five middle caudal vertebrae appear rectangular in lateral view. Generally, the centrum of the middle caudal vertebrae exhibits a nearly flat anterior articular facet and a posterior facet that is slightly concave, a state that differs from derived titanosaurians in which the middle caudal vertebrae are procoelous (Wilson, 2002; Upchurch et al., 2004). The centrum is only slightly concave laterally and ventrally and is subrectangular in shape, similar to the anterior caudal vertebrae described above. The anterior and posterior chevron articular facets are not well developed and do not connect by means of a ventrolateral ridge (Fig. 7A, F). The ventral surface is smooth and lacks a longitudinal hollow (Fig. 7H, L). The transverse process is greatly reduced and consists of a laterally facing circular rugosity. Interestingly, the left transverse processes in the articulated middle caudal series consist of small projections originating from the ventral portion of the rounded rugosity, but these features are not preserved on the right side (Fig. 7B). It is likely that this represents the normal decrease in size of the transverse processes along the caudal series and is asymmetrically preserved. The dorsal part of the circular rugosity is represented by a weakly developed tubercle (Fig. 7C–E, I). The ventrally reduced transverse process and dorsally developed tubercle in middle caudal vertebrae are well developed in the derived titanosaurian *Baurutitan britoi* and less so in *Alamosaurus sanjuanensis* (Kellner et al., 2005). Kellner et al. (2005) suggests that the dorsal tubercle is homologous with a similar tubercle on the transverse process in anterior caudal vertebrae; however, other titanosaurians (e.g., *Saltasaurus loricatus* and *Neuqeunsaurus australis*) do not exhibit the tubercle on the transverse process of anterior caudal vertebrae. Moreover, *Epacthosaurus* and *Gondwanatitan* both exhibit "lateral ridges" (Salgado et al., 1997:27) at the approximate location indicated by Kellner et al. (2005). Whether the lateral ridges and the dorsal tubercle are homologous remains unclear. *Rukwatitan* exhibits a condition similar to that in *Baurutitan,* with the tubercle less developed in more anterior caudals in the former. The neural arch is positioned anteriorly on the centrum, similar to the condition observed in the more anterior vertebrae within the caudal series. The neural spine is transversely compressed, anteroposteriorly expanded, and canted posterodorsally. The spinoprezygapophyseal and spinopostzygapopyhseal laminae of the neural arch are only weakly developed, but prespinal and postspinal laminae are well developed. As such, the pre- and postspinal fossae are present and ventrally bounded by short intraprezygapophyseal and intrapostzygapophyseal laminae, respectively (Fig. 7D, E). The prezygapophysis extends slightly past the anterior end of the centrum. The prezygapophyseal facet is oval, flat, and steeply inclined dorsomedially. The postzygapophysis overhangs the posterior third of the centrum and is oval and slightly concave. A weakly developed postzygapophyseal centrodiapophyseal/spinodiapophyseal fossa (Wilson et al., 2011) is present on the base of the neural spine just anterior to the postzygapophysis (Fig. 7A).

Ribs

Multiple cervical ribs have been preserved and are fused with their respective cervical vertebrae (Figs. 4, 5). Cervical ribs associated with the posterior cervical series are elongate and extend beyond the succeeding vertebra, with rib shafts positioned immediately ventral relative to the shaft of succeeding cervical ribs. The cervical rib of the PCV is reduced such that the rib shaft only extends minimally from the capitulotubercular contacts. Many of the cervical ribs have been recovered or prepared in discrete pieces that were in articulation and close association. The anterior projection of the cervical rib is dorsoventrally flattened and only extends to the posterior margin of the condyle (Fig. 4E, F). This differs from the condition in *Malawisaurus* in which the anterior projection extends to the anterior margin of the condyle in the posterior cervical series (Gomani, 2005:fig. 9). The proximal dorsomedial surface of the cervical rib possesses multiple shallow, pneumatic excavations. The cross-sectional shape of the rib shaft trends from a dorsoventrally compressed plank proximally to rod-like distally.

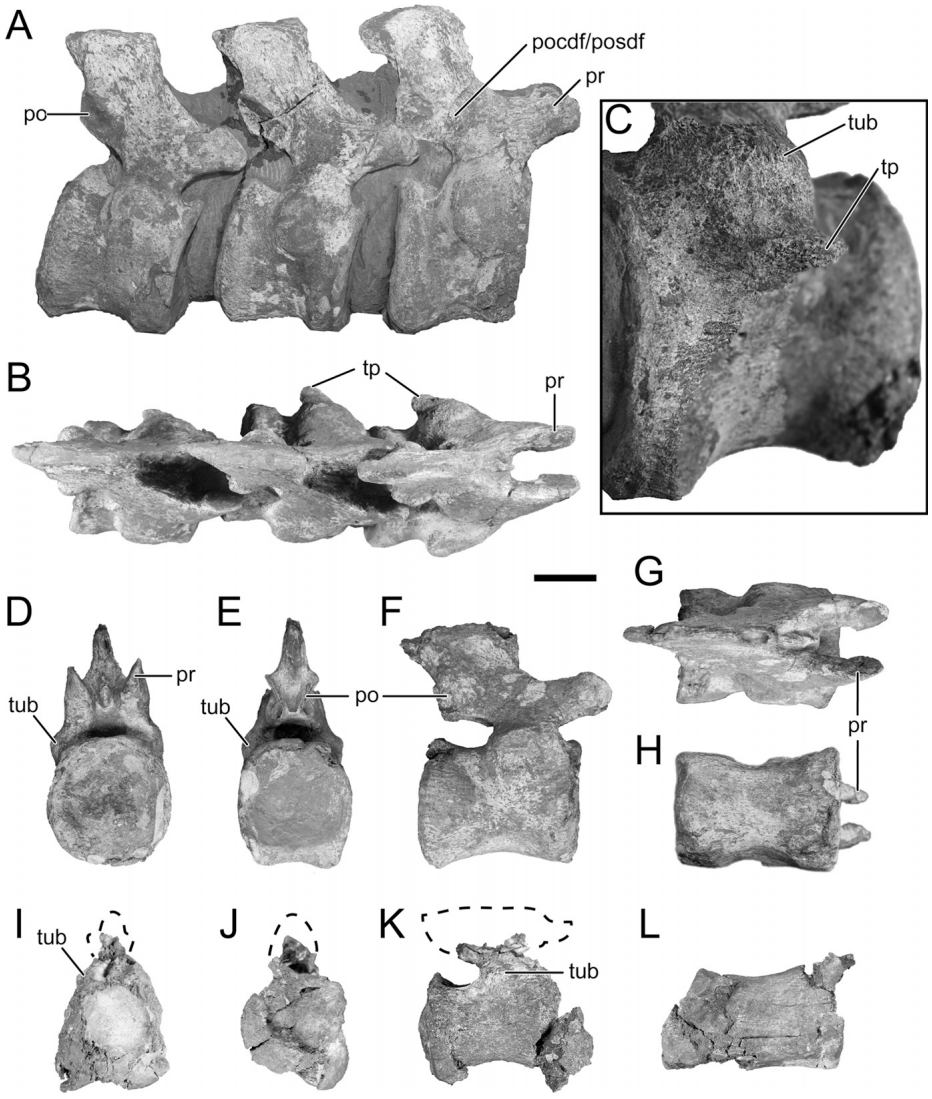

FIGURE 7. Middle caudal vertebrae of *Rukwatitan bisepultus* (RRBP 07409). **A**–**C**, articulated series of three middle caudal vertebrae; **A**, right lateral; **B**, dorsal; and **C**, last caudal vertebra of the series in left anterolateral views. **D**–**H**, isolated middle caudal vertebra; **D**, anterior; **E**, posterior; **F**, right lateral; **G**, dorsal; and **H**, ventral views. **I**–**L**, isolated distal middle caudal; **I**, anterior; **J**, posterior; **K**, right lateral; and **L**, ventral views. Anterior is to the right in **A**–**B**, **F**–**H**, and **K**–**L**. **Abbreviations**: **po**, postzygapophysis; **pocdf/posdf**, postzygapophyseal centrodiapophyseal/spinodiapophyseal fossa; **pr**, prezygapophysis; **tp**, transverse process; **tub**, tubercle. Scale bar equals 5 cm.

Multiple disarticulated dorsal ribs have been recovered (Fig. 2A), but the majority of these elements do not preserve proximal or distal ends. Three partial left anterior dorsal ribs were recovered in close association with the left scapular blade, and a right posterior dorsal rib preserving the capitulum, tuberculum, and proximal region of the shaft was also recovered (Fig. 8A–D). Of the three preserved anterior dorsal ribs, one preserves the majority of the proximal end albeit with slight erosion of the tuberculum and partial capitulum (Fig. 8A, B). Camellate texture can be seen due to the erosional surface along the tuberculum and seems to be present proximally but not within the shaft distally. The capitulum and tuberculum are widely separated by a capitulotubercular web that exhibits multiple, shallow pneumatic fossae across its medial surface (Fig. 8B). Proximally at this level, the rib moderately bulges out laterally before becoming transversely compressed along the shaft. Generally, the cross-sections of the recovered partial dorsal ribs are transversely compressed and plank-like throughout the length, typical of titanosauriforms (Wilson, 2002).

The proximal third of a right posterior dorsal rib (Fig. 8C, D) is well preserved, with the exception of slight erosion on the surface of the capitulum and tuberculum. An acute angle separates the supporting axes of capitulum and tuberculum, indicating a posterior position of the rib along the vertebral column. There is a slight 'kink' in the rib shaft immediately distal to the junction of the capitular and tubercular axes, with the remainder of the rib shaft being transversely expanded and plank-like. A single, large pneumatic foramen pierces the shaft at the base of the capitulotubercular web (Fig. 8D). Pneumatic anterior dorsal ribs are common among titanosauriforms (Wilson and Sereno, 1998; Wilson, 2002). Although the extent and patterning of pneumatic features in posterior dorsal ribs remain relatively unknown (Wilson and Sereno, 1998; Wilson, 2002; Wedel, 2003), pneumaticity within this region is minimally present in *Malawisaurus* and *Diamantinasaurus* (Gomani, 2005; Hocknull et al., 2009).

Chevron

One partial chevron blade and a single complete chevron were recovered, with the latter being well preserved (Fig. 8E–G). The partial chevron blade is larger and assumed to be from a more anterior position, but is otherwise unremarkable. The complete chevron is deeply divided to approximately one-half of the total length and unforked (Fig. 8E, F), as is typical in titanosaurians (Wilson, 2002). The division between the rami forms a narrow 'V' shape, and the articular ends are not joined together by a crus (Fig. 8E, G). The flat articular facets are subtriangular and

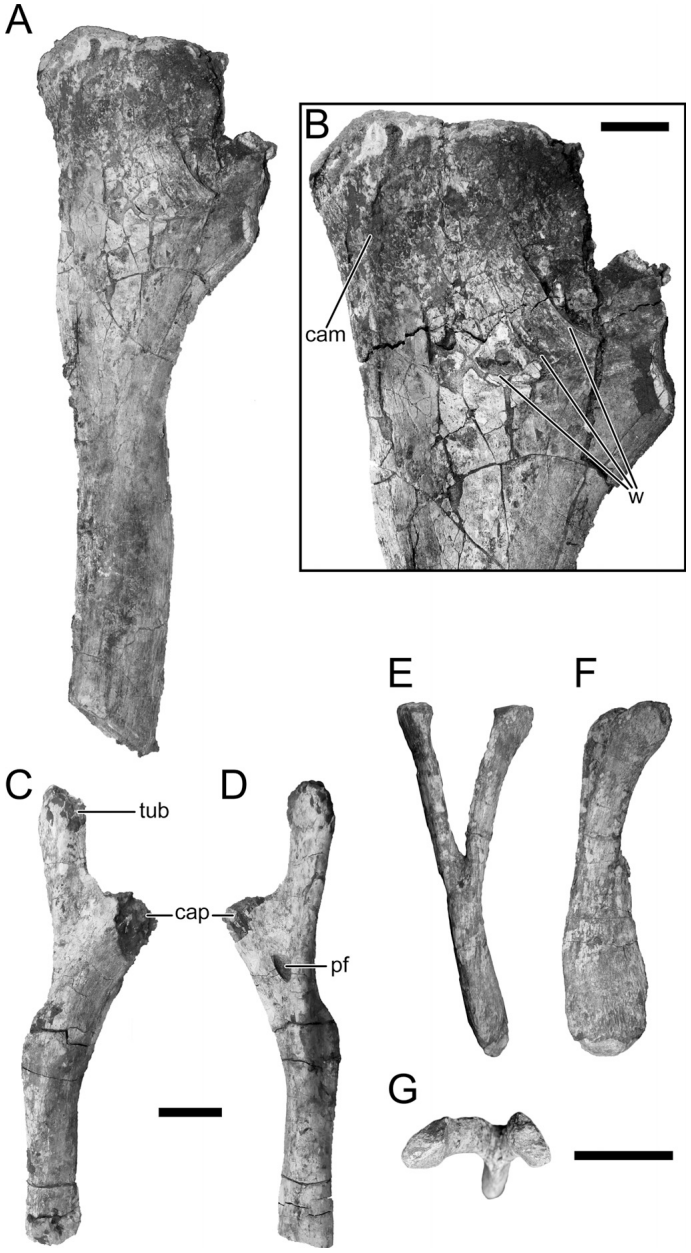

FIGURE 8. Dorsal rib and chevron morphology of *Rukwatitan bisepultus* (RRBP 07409). **A**–**B**, anterior dorsal rib; **A**, posterior; and **B**, close-up views, with **B** illustrating the detailed morphology of the capitulotubercular web. **C**–**D**, posterior dorsal rib; **C**, anterior; and **D**, posterior views. **E**–**G**, chevron; **E**, anterior; **F**, left lateral; and **G**, dorsal views. Anterior is toward the top in **G**. **Abbreviations**: **cam**, camellate texture; **cap**, capitulum; **pf**, pneumatic foramen; **tub**, tuberculum; **w**, capitulotubercular webbing. Scale bars equal 5 cm.

face posteromedially. The distal half of the chevron is laterally compressed and expanded anteroposteriorly.

Pectoral Girdle

Pectoral elements of *Rukwatitan* are currently limited to the left scapular blade and portions of both coracoids (Fig. 9). Unremarkable portions of the right scapula(?) were recovered, but are otherwise heavily eroded and extremely fragmentary. The left scapular blade is well preserved and is associated with the

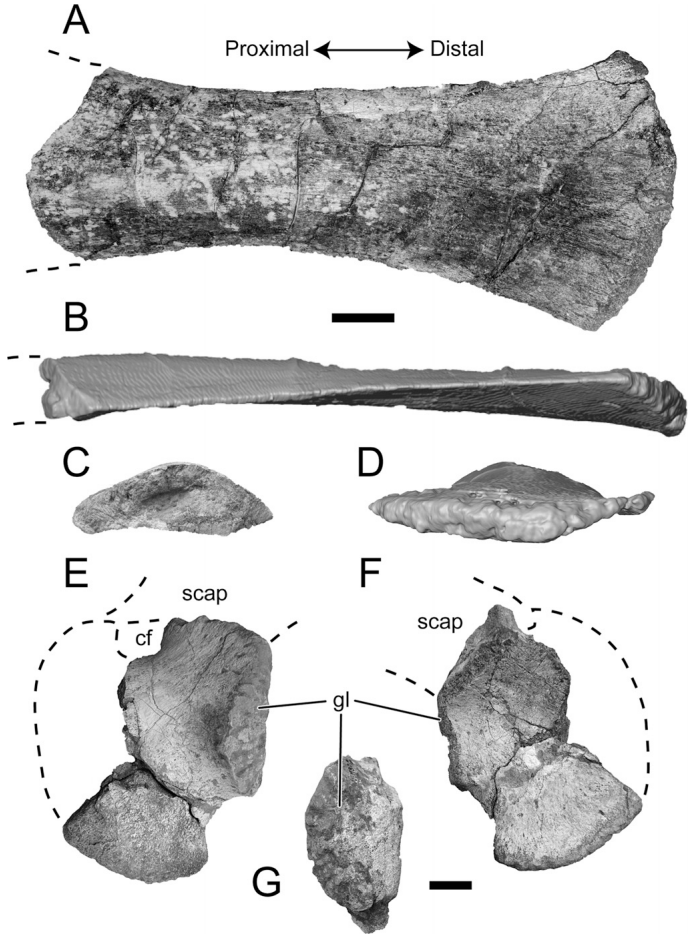

FIGURE 9. Left scapular blade morphology and left coracoid of *Rukwatitan bisepultus* (RRBP 07409). **A**–**D**, left scapular blade; **A**, lateral; **B**, ventral; **C**, proximal; and **D**, distal views. **B** and **D** are digital reconstructions based on computed tomography (CT) scans. **E**–**G**, left coracoid; **E**, lateral; **F**, medial; and **G**, posterior views. **Abbreviations**: **cf**, coracoid foramen; **gl**, glenoid; **scap**, scapular articulation. Scale bars equal 5 cm.

three proximal dorsal ribs noted above (Fig. 9A–D). The partial left coracoid preserves part of the coracoid foramen, partial scapular and glenoid articular surfaces, and the anteroventral aspect of the element. The right coracoid exhibits a slightly better scapular articular surface, but the remainder has been eroded away and weathered. As such, only the left coracoid will be described below.

Scapula—The orientation of the scapula for the description assumes that the long axis of the blade is positioned along the anteroposterior axis. The scapular blade is generally thin, especially along the edges. The blade expands distally along the dorsal and ventral margins, with the ventral edge exhibiting a slightly more developed concavity than the dorsal margin (Fig. 9A). Proximally, the blade is medially concave and flattens distally. The scapular blade exhibits a roughly 'D'-shaped cross-section near the incomplete proximal end that is common in most neosauropods (Wilson, 2002). In cross-sectional view (Fig. 9C), the ventral margin tapers to an acute angle and the dorsal margin is rounded. The distal margin is rugose, more so laterally than medially (Fig. 9D). The medial surface of the preserved scapular blade does not exhibit the ventral or dorsal ridges that are observed in *Lirainosaurus astibiae* and several other titanosaurians (Sanz et al., 1999).

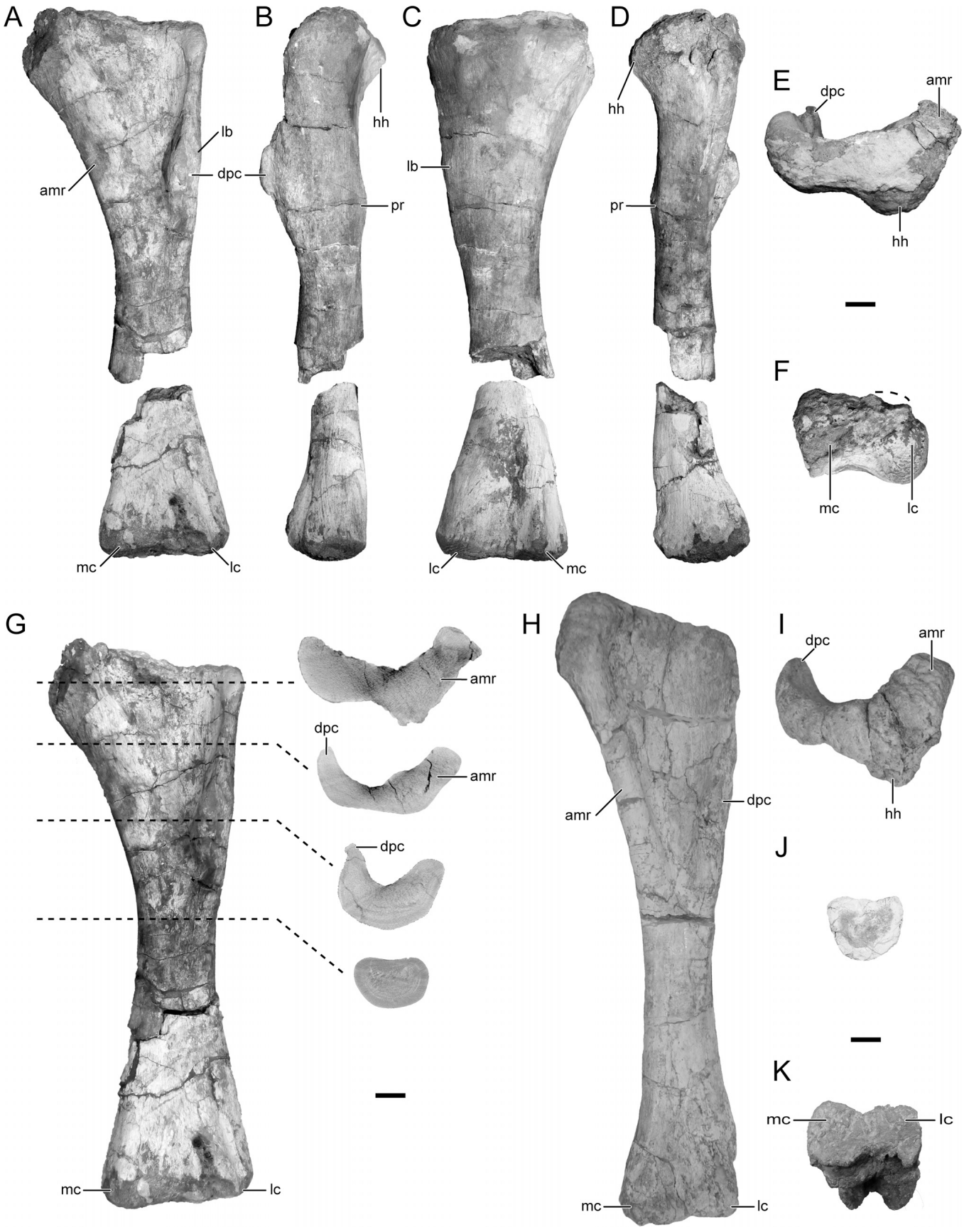
A
lb
amr
dpc
mc
lc
B
hh
pr
C
lb
lc
mc
D
hh
pr
E
dpc
amr
hh
F
mc
lc
G
amr
dpc
amr
dpc
mc
lc
H
amr
dpc
mc
lc
I
dpc
amr
hh
J
K
mc
lc

Coracoid—The orientation of the coracoid for the description assumes that its glenoid contribution faces posteriorly. Because the anterodorsal portion of the coracoid is not preserved, the overall shape cannot confidently be described as either oval or rectangular (e.g., character 156 of Wilson, 2002). The presence of fortuitous breaks, eroded surfaces, and CT scan data reveal that the coracoid is not pneumatic as has been interpreted in some derived saltasaurids (e.g., Cerda et al., 2012a). The lateral surface is gently convex, with the medial surface being gently concave. Moderate texturing occurs near the scapular and glenoid articular surfaces. The scapulocoracoid is unfused, and coracoid foramen is inferred to be patent. The partial glenoid is oval-shaped posteriorly, with a continuing surface facing posterolaterally (Fig. 9E, G). There is no prominent, hook-like infraglenoid lip as observed in derived titanosaurians such as *Opisthocoelicaudia skarzynskii* (Fig. 9E, F; Borsuk-Bialynicka, 1977:pls. 7–8). The ventral corner of the coracoid is rounded, and the distance between the glenoid and the ventral corner is much longer than in *Malawisaurus dixeyi* (Gomani, 2005:fig. 19), *Tapuiasaurus macedoi* (Zaher et al., 2011:fig. 5), and *Rapetosaurus krausei* (Curry Rogers, 2009:fig. 33). The coracoid appears to have been proximodistally longer and approaching the condition of derived titanosaurians (e.g., saltasaurids; Wilson, 2002), but due to the incomplete nature of the element, this remains a tentative assessment. The partial anteroventral margin is gently curved and does not appear rectangular as in more derived titanosaurians (Upchurch, 1998; Wilson, 2002; D'Emic, 2012).

Humerus

The left humerus (Fig. 10A–G) of the holotype of *Rukwatitan* is well preserved, although the recovered distal end was displaced (approximately 1.5 m) from the proximal end (see Fig. 2). In anterior view, the humerus is relatively slender at midshaft, with moderately expanded proximal and weakly expanded distal ends. The humeral head is positioned medially on the proximal end and extends to an equivalent position with the proximal end of the deltopectoral crest (Fig. 10A–C, E). The proximal and lateral margins of the humerus form a squared-off corner (Fig. 10A), a feature exhibited by many titanosaurians and variably present within the more inclusive titanosauriforms (Upchurch, 1999; Wilson, 2002; Upchurch et al., 2004; Mannion and Calvo, 2011; D'Emic, 2012; Mannion et al., 2013). The humeral head extends posteriorly and overhangs the posterior margin of the humeral shaft and continues laterally as a lip (Fig. 10B, D). The proximal and posterior margins of the humeral head curve sharply to form this overhanging portion. A deep coracobrachialis fossa is situated on the anterior surface of the proximal half of the humerus (Fig. 10A, G). The fossa is prominent due to the anterior extension of the deltopectoral crest on the lateral margin of the humerus and anteromedial extension of the medial ridge. This fossa is clearly visible in proximal and cross-sectional views (Fig. 10E, G) and is even more apparent in the humerus here referred to *Rukwatitan* (RRBP 03151; Fig. 10I). Within the coracobrachialis fossa, a rugose bump (m. coracobrachialis brevis attachment; Borsuk-Bialynicka, 1977) is positioned on the proximomedial surface. The deltopectoral crest is represented by a ridge that spans from the proximal end through approximately half of the humeral length and exhibits a moderate medial expansion along the distal half (Fig. 10A). The anterior-most margin of the deltopectoral crest curves slightly laterally (Fig. 10G). The proximal third of the posterior surface of the humerus is slightly concave, bounded by the lip along the proximal margin and a prominent posterior protuberance at approximately one-third of the distance along the shaft (Fig. 10B, D). An incipient lateral bulge is positioned on the lateral surface of the humerus at the level of the deltopectoral crest and slightly more proximal than the posterior protuberance (Fig. 10A–C), similar to the condition in derived titanosaurians but not *Malawisaurus* (D'Emic, 2012). The cross-section at the midshaft is subquadrangular, with flattened anterior, posterior, lateral, and medial surfaces (Fig. 10G, J). This cross-sectional shape differs from other sauropods where the cross-sectional outline is either elliptical (most sauropods) or round (e.g., Rebbachisauridae, Wilson, 2002; however, see Mannion et al., 2012:table 4) and is here considered an autapomorphy of *Rukwatitan.* This subquadrangular cross-section is even more pronounced in the referred humerus (RRBP 03151; Fig. 10J). The distal humerus expands slightly along the transverse axis, with no evidence of prominent epicondyles. The distal end is gently convex on both medial and lateral condyles; however, the distinction between the two condyles is subtle. The medial condyle projects slightly anterior relatively to the shaft, whereas the lateral condyle is in-line with the longitudinal axis (Fig. 10B, D, F). In more derived titanosaurians, the distal condyles are distinct and extend anteriorly from the shaft, whereas the condition in *Rukwatitan* only incipiently exhibits this condition (Wilson, 2002).

An isolated right humerus (RRBP 03151) from a different locality is also referred to *Rukwatitan*. Similar in overall morphology (Fig. 10H–K), the specimen is more elongate (by approximately 10%) and slightly more gracile than the holotype humerus. The slenderness of the referred specimen is similar to the derived titanosaurian *Muyelensaurus pecheni* (Calvo et al., 2007:fig. 12b), except that the coracobrachialis fossa and proximal portion is more prominent in *Rukwatitan.* The element is well preserved and missing only the posterior and most distal margins of the medial and lateral condyles. The deep coracobrachialis fossa is more developed than on the holotype specimen due to an accentuated anteromedial ridge. A deep coracobrachialis fossa is also described on humeri of the Late Cretaceous *Gondwanatitan faustoi* and *Argyrosaurus superbus* (Kellner and Azevedo, 1999; Mannion and Otero, 2012); however, the fossa in *Rukwatitan* differs from the condition observed in these taxa. The anteromedial ridge in *Argyrosaurus* persists for most of the humeral length and the fossa appears more open proximally (Mannion and Otero, 2012:fig. 2c). In *Rukwatitan*, the anteromedial ridge ends roughly halfway along the length of the humerus, and the coracobrachialis fossa is more constricted by the anteromedial ridge and pronounced deltopectoral crest. The fossa in *Gondwanatitan* is bounded laterally by the anteromedially curved deltopectoral crest. The deltopectoral crest in *Rukwatitan* does not curve medially but rather projects anteriorly. Therefore, *Rukwatitan* is unique in having a deep coracobrachialis fossa that is bounded by a combination of a strong anteriorly projecting deltopectoral crest and a strong anteromedial ridge that only persists through the proximal half of the humerus.

Ulna

The right ulna (Fig. 11) is partially preserved and consists of the shaft and proximal expansions, whereas the proximal

← FIGURE 10. Left humerus (RRBP 07409) and right referred humerus (RRBP 03151) of *Rukwatitan bisepultus.* **A–G**, left humerus; **A**, anterior; **B**, lateral; **C**, posterior; **D**, medial; **E**, proximal; **F**, distal; and **G**, series of cross-sectional views. Cross-sections in **G** are digital reconstructions based on computed tomography (CT) scans. **H–K**, referred right humerus (images reversed); **H**, anterior; **I**, proximal; **J**, cross-sectional; and **K**, distal views. Anterior is to the top in **E–G** and **I–K. Abbreviations**: **amr**, anteromedial ridge; **dpc**, deltopectoral crest; **hh**, humeral head; **lb**, lateral bulge; **lc**, lateral condyle; **mc**, medial condyle; **pr**, protuberance. Scale bar equals 5 cm.

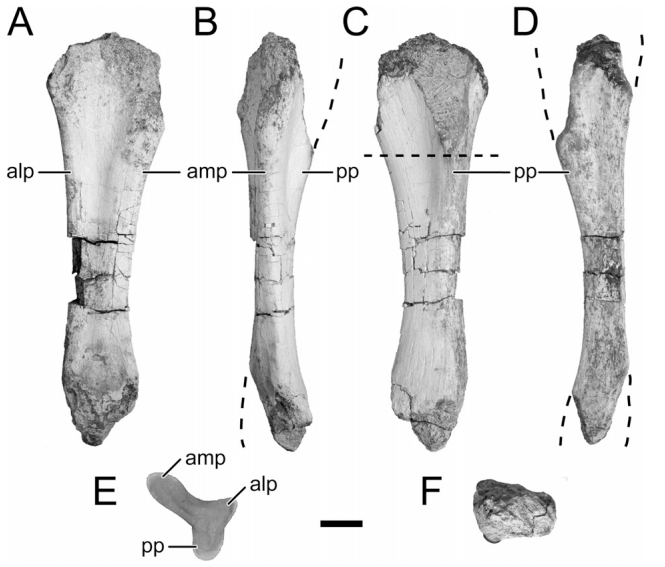

FIGURE 11. Right ulna of *Rukwatitan bisepultus* (RRBP 07409). **A**, anterolateral; **B**, anteromedial; **C**, posteromedial; **D**, posterolateral; **E**, cross-sectional; and **F**, distal views. **E** is a digital reconstruction based on computed tomography (CT) scans. Anterior is to the top in **E** and **F**. Dotted line in **C** represents level of which **E** was taken from CT scans. **Abbreviations**: **alp**, anterolateral process; **amp**, anteromedial process; **pp**, posterior process. Scale bar equals 5 cm.

articular surface, olecranon process, and distal end are not preserved. The ulna is generally slender and moderately expanded proximally such that the three proximal processes form an asymmetrical, tri-lobed cross-section (Fig. 11E). Although the anteromedial process is more pronounced than either of the anterolateral or olecranon/posterior processes, all three are relatively slender. The anteromedial and anterolateral processes form a wide groove along the anterolateral surface to accommodate the radius. Midway along the shaft within this groove lies a low ridge that grades onto the distal portion of the element (Fig. 11A). Less pronounced grooves are present between the anteromedial and posterior processes and between the anterolateral and posterior processes. The anteromedial process continues as a low ridge that persists more distally than do the other two processes. The medial surface of the shaft bows distally. The posterior surface retains a relatively straight margin throughout its length. The distal portion of the ulna is not preserved, terminating near the distal radial articulation. In distal view, the preserved ulnar shaft exhibits a subrectangular cross-section (Fig. 11F).

Pelvic Girdle

The pelvic girdle of *Rukwatitan* is represented by a nearly complete left ilium and the proximal portion of the right pubis (Fig. 12). Although both elements are well preserved, the dorsal margin of the iliac crest and the distal portion of the pubis were eroded subsequent to the initial depositional event. The left ilium was recovered within the overbank mudstone (Fig. 2A). By contrast, the proximal right pubis was recovered within an eroded block of the channel sandstone, suggesting that it was originally eroded at some point in the past and redeposited within the channel facies. The ilium contributes the largest proportion of the acetabular rim, with an elongated pubic peduncle and a reduced ischial peduncle. The ischium can be inferred to contribute a larger portion of the acetabular rim than the pubis (Fig. 12A, H).

Ilium—The dorsal margin of the ilium is not preserved. It appears that the ilium is not pneumatic due to the lack of internal camellate texturing or large internal cells either through direct observations of eroded surfaces or via CT scans. Several ilia have been reported or described, with internal morphology consistent with pneumatic bone in the titanosauriform *Euhelopus zdanskyi* (Wilson and Upchurch, 2009) and several derived titanosaurians (*Saltasaurus loricatus*, *Rocasaurus muniozi*, and *Neuquensaurus australis*, Cerda et al., 2012a; *Epachhosaurus sciuttoi*, Martínez et al., 2004; *Lirainosaurus*, Sanz et al., 1999; *Sonidosaurus saihangaobiensis*, Xu et al., 2006; *Diamantinasaurus matildae*, Hocknull et al., 2009; *Alamosaurus sanjuanensis*, Woodward and Lehman, 2009). In these forms, the extent of putative iliac pneumaticity is generally limited in the dorsal region of the anterior and medial iliac blades, neither of which is preserved in *Rukwatitan.* The preacetabular iliac blade is semicircular and robust anteriorly (Fig. 12B), as in ilia of most titanosauriforms (Upchurch, 1998; Wilson and Sereno, 1998; Wilson, 2002). The preacetabular process flares anterolaterally (Fig. 12C, F) like most titanosauriforms, but not to the extent that it is perpendicular to the long axis of the body as exhibited by derived titanosaurians (Salgado et al., 1997; Wilson, 2002). The iliac blade thins towards the middle section of the element, with a rugose surface texture apparent along the dorsal margin at both anterior and posterior ends. The preacetabular process is slightly concave ventrally but flattens along the anteroventral edge of the element. The relatively long postacetabular process is nearly level with the ischial peduncle, but delineated from it by a small notch (Fig. 12A, D, F). The pubic peduncle is elongate and extends perpendicular to the long axis of the ilium. The articular surface for the pubis is teardrop-shaped, with the 'tail' of the teardrop curving posteromedially (Fig. 12F). The lateral margin of the pubic peduncle is markedly expanded along the anteroposterior axis, with a slight lateral bulge (Fig. 12A, F). The anterior and posterior margins of the pubic peduncle meet to form a sharp medial ridge that spans the length of the peduncle. The posteriorly curved, teardrop-shaped articular surface and relatively slender pubic peduncle of *Rukwatitan* contrasts with many titanosauriforms wherein the pubic peduncle is transversely expanded and slightly crescent-shaped. In more derived titanosaurians such as *Neuquensaurus australis* (Salgado et al., 2005), the robust pubic peduncle is teardrop-shaped, with only a minimal posterior curvature. Moreover, *Gondwanatitan faustoi* (Kellner and Azevedo, 1999:fig. 18) also exhibits a significant transverse expansion of the pubic peduncle. The titanosaurian pelves described in Campos and Kellner (1999) are also similar to the condition in *Gondwanatitan*. Thus, *Rukwatitan* is unique in exhibiting a slender, curved, teardrop-shaped pubic peduncle that is less transversely expanded than in derived forms. By contrast, the ischial peduncle is low, rounded, and somewhat crescent-shaped, with an anterolaterally facing concavity (Fig. 12F).

Pubis—The proximal end of the right pubis is preserved, with slight surface erosion on the articular surfaces for both the ilium and ischium (Fig. 12G–L). The acetabular margin and oval obturator foramen are well defined (Fig. 12G, H), with the latter entirely enclosed by surrounding bone. The obturator foramen is positioned ventral to the posterior aspect of the acetabular margin. The long axis of the obturator foramen appears to be slightly offset from the long axis of the pubis. This would differ from *Andesaurus* and other titanosauriforms in which the long axis of the obturator foramen is in-line with the long axis of the pubic shaft (Mannion and Calvo, 2011). This inference is tentative owing to the absence of the distal pubic shaft and its exact orientation relative to the body and obturator foramen. The cross-section along the fracture plane is thin and teardrop-shaped, with

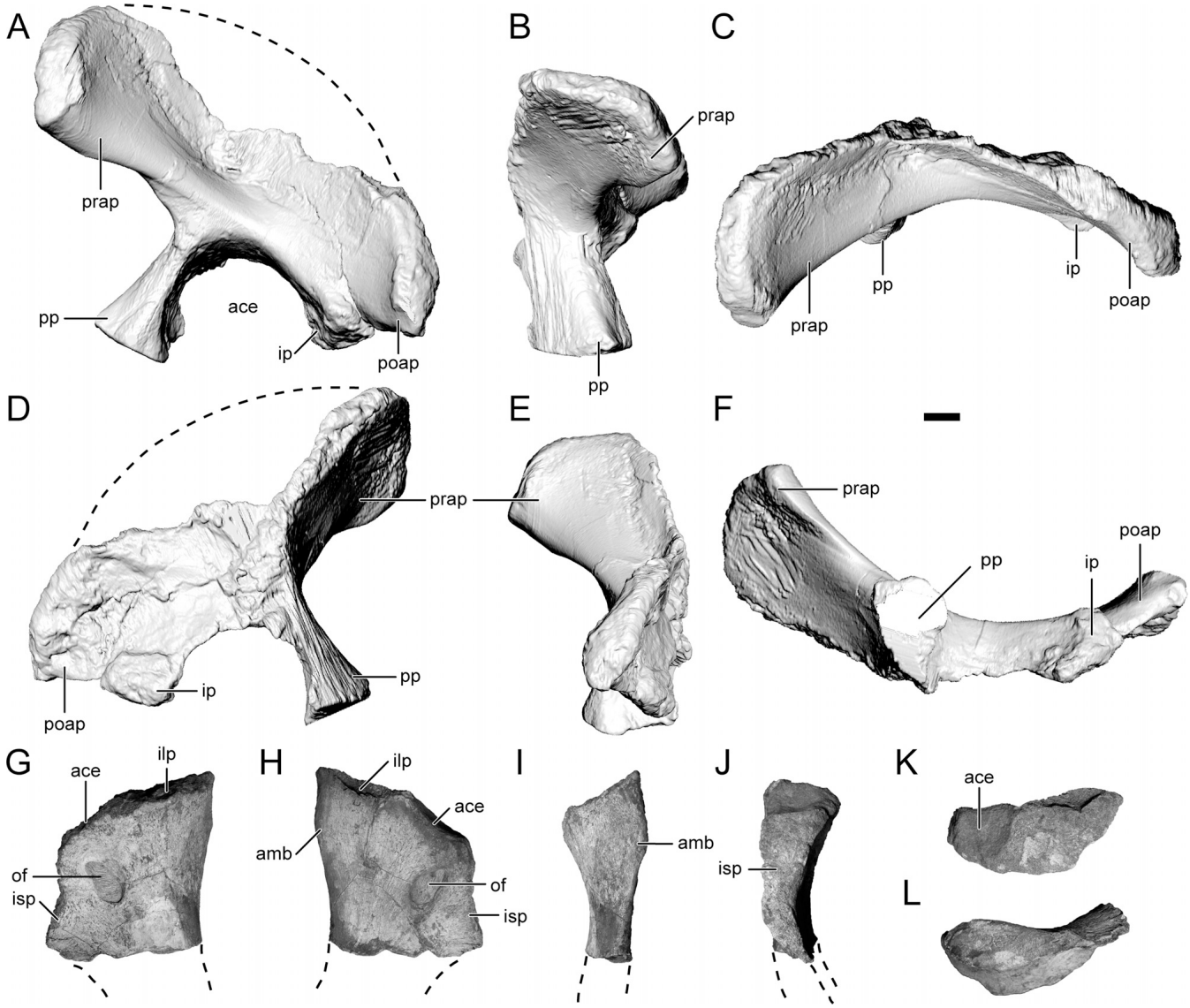

FIGURE 12. Pelvic girdle of *Rukwatitan bisepultus* (RRBP 07409). **A**–**F**, left ilium; **A**, lateral; **B**, anterior; **C**, dorsal; **D**, medial; **E**, posterior; and **F**, ventral views. Ilium images are digital reconstructions based on computed tomography (CT) scans. **G**–**L**, right pubis; **G**, lateral; **H**, medial; **I**, anterior; **J**, posterior; **K**, dorsal; and **L**, ventral views. **Abbreviations**: **ace**, acetabulum; **amb**, pubic ambiens; **ilp**, iliac peduncle; **ip**, ischial peduncle (of ilium); **isp**, ischial peduncle (of pubis); **of**, obturator foramen; **poap**, postacetabular process; **pp**, pubic peduncle; **prap**, preacetabular process. Scale bar equals 5 cm.

the wider part positioned medially. The pubic ambiens process is weakly developed, short, and slightly angled with respect to the anterior margin of the pubis. The articular surface for the ilium is broad, flat, and triangular, with a convex anterior surface. This surface grades into the slightly curved acetabular margin posteriorly. The ischial articular surface faces posterodorsally and forms a steep angle relative to the acetabular margin (Fig. 12H). The ischial articulation sweeps laterally before abruptly ending at the incomplete distal end.

PHYLOGENETIC RELATIONSHIPS

The phylogenetic affinity of *Rukwatitan* was assessed using the character definitions and data matrix of Wilson (2002), with modifications from the Zaher et al. (2011) analysis of *Tapuiasaurus macedoi*. Zaher et al. (2011) also included the Early–middle Cretaceous somphospondylans *Diamantinasaurus matildae* (Hocknull et al., 2009), *Tangvayosaurus hoffeti* (Allain et al., 1999), and *Phuwiangosaurus sirindhornae* (Suteethorn et al., 2009). Additionally, *Andesaurus delgadoi* (Calvo and Bonaparte, 1991) was incorporated into the data matrix based on redescriptions from Mannion and Calvo (2011). *Andesaurus* serves as a key taxon in defining Titanosauria (*Andesaurus delgadoi*, *Saltasaurus loricatus*, their most recent common ancestor and all descendants; Bonaparte and Coria, 1993; Wilson and Upchurch, 2003; D'Emic, 2012; Mannion et al., 2013) and for explicitly testing the titanosaurian affinities of *Rukwatitan.* The addition of *Rukwatitan* to this matrix brings the total number of taxa to 35 (see Supplementary Data, Appendix S1). Zaher et al. (2011) added 12 cranial characters to this matrix based on information from Upchurch et al. (2004), Curry Rogers (2005), and Wilson (2005), resulting in a total of 246 characters (see Supplementary

Data, Appendix S2). In addition to adding the novel scorings for *Rukwatitan*, the current phylogenetic analyses include modified scorings for *Euhelopus zdanskyi* (Wilson and Upchurch, 2009; Zaher et al., 2011). Characters 8, 37, 64, 66, and 198 were treated both as ordered (as originally in Wilson, 2002) and unordered states. However, the topologies of the ordered and unordered analyses are indistinguishable from one another. A total of 51 characters (approximately 21% of the total characters, and 30% of the postcranial characters) were scored for *Rukwatitan*. Although the total number of scored characters may seem low (79% missing data from the total characters), the variety of scored characters represents several different regions of the skeleton, including axial and both appendicular regions.

Parsimony analyses were conducted in PAUP version 4.0b10 (Swofford, 2003) using random addition and tree-bisection-reconnection options within the heuristic search framework and was cycled for 10,000 repetitions. Both bootstrap and jackknife resampling analyses were performed to calculate nodal support values (Felsenstein, 1985; Farris et al., 1996). In addition, Bremer support values were generated (Bremer, 1994). Each resampling analysis ran 1000 replicates using the heuristic search algorithm with random addition and tree-bisection-reconnection options in PAUP version 4.0b10 (Swofford, 2003). Jackknife values over 50% are reported in Figure 13, whereas the bootstrap values can be accessed from Supplemental Data. The heuristic search produced 24 most parsimonious trees (MPTs) with a length of 484 steps. The strict consensus effort results in a mostly resolved tree, except for polytomies within the Rebbachisauridae and *Tangvayosaurus*, *Andesaurus*, *Rukwatitan*, *Malawisaurus*, and more derived titanosaurians nodes. The majority-rule consensus tree maintains the polytomies within Rebbachisauridae and with *Tangvayosaurus*, *Andesaurus*, and more derived titanosaurians (Fig. 13A). Not surprisingly the consensus trees are generally consistent with the tree topologies as promoted by both Wilson (2002) and Zaher et al. (2011). *Rukwatitan* is placed outside the clade formed by *Malawisaurus* and more nested titanosaurians (hereafter Lithostrotia; sensu Upchurch et al., 2004; D'Emic, 2012) in 63% of the 24 MPTs, whereas the latter grouping is seen in 75% of the 24 MPTs. A suite of characters (indicated by the bracketed numbers; see Character List in Appendix S2) support the relationship of *Rukwatitan* with Lithostrotia, including undivided pleurocoels on cervical vertebrae [83], procoelous anterior caudal vertebrae [118], and acromial edge of the distal scapular blade not expanded [152]. However, several of these characters have also been identified elsewhere within Sauropoda: procoelous anterior caudal vertebrae are found in some diplodocoids (e.g., *Diplodocus*) and non-neosauropods such as *Mamenchisaurus*, *Bellusaurus*, and *Turiasaurus* (Young, 1954; Dong, 1990; Royo-Torres et al., 2006), and an unexpanded acromial edge of the distal scapular blade is found in some non-neosauropods, diplodocoids, and *Euhelopus* (Wilson, 2002; Wilson and Upchurch, 2009; D'Emic, 2012). Thus, the features listed that support *Rukwatitan* with Lithostrotia as a clade are informative when viewed within the context of Titanosauriformes. *Rukwatitan* is positioned among basal titanosaurians and is excluded from Lithostrotia by the absence of a ventral longitudinal hollow on the caudal vertebrae [132], a character that has also been used to help diagnose titanosaurians (Wilson, 2002; Curry Rogers, 2005; D'Emic, 2012).

In addition to the parsimony-based phylogenetic analysis discussed above, a Bayesian phylogenetic analysis was performed to evaluate the relationship of *Rukwatitan* within a model-based framework to provide a complementary assessment and perhaps to aid in resolving the ambiguities (e.g., low Bremer and jackknife values; Fig. 13A) surrounding the basal titanosaurian area of the trees produced from the parsimony analysis. Only a handful of Bayesian analyses have incorporated morphological data

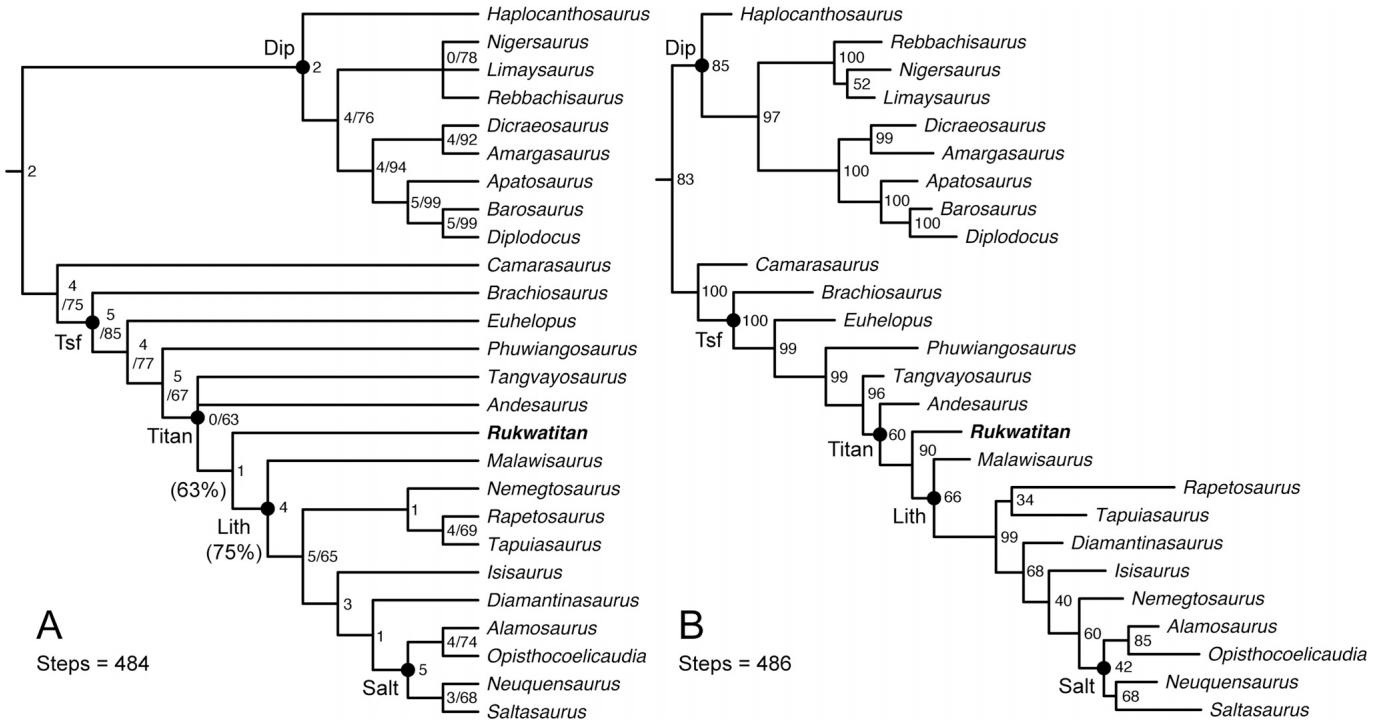

FIGURE 13. Results of the parsimony and Bayesian phylogenetic analyses. **A**, the 24 most parsimonious trees reduced into a majority-rule consensus tree, with frequency of clades (>50%) in parentheses and Bremer and jackknife (>50%) nodal support values where applicable; **B**, resultant Bayesian topology from the gamma rates model with posterior probabilities at each node. **Abbreviations**: **Dip**, Diplodocoidea; **Lith**, Lithostrotia; **Salt**, Saltasauridae; **Titan,** Titanosauria; **Tsf**, Titanosauriformes.

in combination with molecular data or used morphological data exclusively. For examples of combined data sets, see Nylander et al. (2004), Lee (2005), Wiens et al. (2005, 2010), Magallón, (2010), Pyron (2011), Ronquist et al. (2012), and Wood et al. (2013), and for exclusively morphological data sets, see Lewis (2001), Müller and Reisz (2006), Clarke and Middleton (2008), Snively and Cox (2008), Prieto-Márquez (2010), Kear and Barrett (2011), and Lee and Worthy (2012), with the latter six studies focused on morphological data exclusively within vertebrate paleontology. The Bayesian approach used herein generally follows the analytical protocol of Nylander et al. (2004) and Prieto-Márquez (2010), in which the Mk model (Markov model with 'k' number of observed states; Lewis, 2001) is used as the standard likelihood model for morphological data in MrBayes 3.1.2 (Huelsenbeck and Ronquist, 2001; Ronquist and Huelsenbeck, 2003). As addressed by Müller and Reisz (2006) and Prieto-Márquez (2010), the Mk model is better suited when autapomorphies are included in the data set in order to prevent biased estimation of the branch length parameters, because this in turn may influence tree topology (Lewis, 2001; Müller and Reisz, 2006). Müller and Reisz (2006) reported only minor differences in branch lengths, posterior probabilities, and taxon placement in analyses that alternatively omitted or included autapomorphies. We included autapomorphies in the present analyses in order to better estimate the branch length parameters (see Appendix 2; Müller and Reisz, 2006; Prieto-Márquez, 2010). Future studies exploring the influence of autapomorphies on the models and topologies are needed to expand upon the Bayesian phylogenetic methodology for morphological data where only variable characters are generally recorded (Lewis, 2001).

The Bayesian analysis was performed using two different models. The first model assumed equal rates of character change (equal-rates model) and the second model assumed variable rates of character change as established by a gamma-shaped distribution parameter (gamma rates model). The default priors in MrBayes 3.1.2 were used, with each analysis continuing through 14,000,000 generations and sampled every 100 generations with 3 chains (1 'cold' chain and 2 'hot' chains sampling the tree space). The first 25% of sampled generations were discarded as the 'burn-in,' with the remaining samples used to construct the consensus tree (the choice of 25% burn-in is the default value for the convergence diagnostics in MrBayes and is usually enough to discard the initial 'climbing' phase before reaching stationarity; Huelsenbeck and Ronquist, 2001; Ronquist and Huelsenbeck, 2003). Both trials reached stationarity early during the runs from both graphical (using the 'sump' command in MrBayes creates a trace plot of the log-likelihoods per sampled generation) and statistical (standard deviation of split frequencies below 0.05) perspectives. Selection of the preferred model may be determined in two ways. The first criterion selects the model with the harmonic mean of the log-likelihoods closest to 0, whereas the second criterion uses the harmonic means from the different models to compute the Bayes factor, a statistic to assess which model is more strongly supported by the data (Kass and Raftery, 1995; Müller and Reisz, 2006). The Bayes factor is twice the difference of the harmonic means from the two models. Any difference greater than 10 indicates a strong difference between the two models, in which case the model with the log-likelihood closest to 0 is the preferred model.

The resultant topologies from both equal and gamma rates Bayesian models are in general agreement, with only minor differences in branch lengths and nodal posterior probabilities. Perhaps most importantly the Bayesian topologies generally agree with the parsimony topology. The harmonic mean of the log-likelihoods of the equal-rates model is −3355.03 and the gamma rates model is −3237.85. Based on log-likelihoods alone, the gamma rates model is preferred over the equal-rates model. The Bayes factor, twice the difference of the harmonic means of the log-likelihood, is equal to 234.36 and suggests that the preference for the gamma rates model is strongly supported. Herein, the Bayesian topology discussed will be based on the gamma rates model and is figured showing all compatible groupings (Fig. 13B; the equal-rates model topology is not figured but the tree file is available in Supplemental Data). The posterior probability for the clade of *Rukwatitan* and Lithostrotia (notably in the same position as in the parsimony analysis) is well supported at 90%, but Lithostrotia is markedly lower at a posterior probability of 66%. The derived titanosaurian clade (to the exclusion of *Rukwatitan* and *Malawisaurus*) has a high posterior probability at 99% (Fig. 13B). This suggests that *Malawisaurus* is only slightly more probable to form a clade with derived titanosaurians than if *Rukwatitan* was grouped with derived titanosaurians or as sister taxon to *Malawisaurus*. The results of the Bayesian analysis indicate some ambiguity in the position of *Rukwatitan* and *Malawisaurus* with respect to derived titanosaurians. This ambiguity is consistent within the parsimony framework, because the addition of one extra step to the tree can place *Rukwatitan* as either sister taxon to *Malawisaurus* or more derived than *Malawisaurus*. Areas of difference between the parsimony and Bayesian topologies include the placement of *Diamantinasaurus*, *Isisaurus*, and *Nemegtosaurus* in the Bayesian analysis (however, note that these taxa are not well supported in their placement with low posterior probabilities of 68%, 40%, and 60%, respectively). In contrast to more recent analyses, *Nemegtosaurus* is no longer positioned among the clade of titanosaurians (e.g., the clade of *Rapetosaurus* and *Tapuiasaurus*, which has a low posterior probability of 34%) best known from well-preserved cranial material (e.g., Zaher et al., 2011:fig. 7). Instead, *Nemegtosaurus* is positioned relatively closer to *Saltasaurus*, the only other taxon of derived titanosaurians in the data matrix that preserves cranial material. Characters that support *Nemegtosaurus* outside of the *Rapetosaurus* and *Tapuiasaurus* clade and more closely related to *Saltasaurus* include basipterygoid process diverging at an angle less than 30° [47], sheet-like basal tubera [48], and deeper, anterior ramus relative to minimum depth of the dentary [55]. Finally, to further evaluate both trees, we calculated the total number of additional steps required to generate the topology for the Bayesian tree within a parsimony framework using Mesquite version 2.75 (Maddison and Maddison, 2011) and then compared the score with the parsimony tree. The number of steps for the Bayesian tree is 486 compared with the 484 steps for the parsimony tree. The main difference between the topologies of the two analyses occurs with regard to the placement of several taxa within Lithostrotia as discussed above. The Bayesian topology is only two steps longer than the parsimony topology. This is generally similar to the results of Müller and Reisz (2006), who reported that topologies of their Bayesian analyses were three to four steps longer than their MPT.

Overall, both the parsimony and Bayesian topologies broadly agree with one another and specifically in the placement of *Rukwatitan* as a basal titanosaurian to the exclusion of lithostrotian titanosaurians (Fig. 13). Interestingly, *Rukwatitan* shares select lithostrotian characters proposed as part of recent efforts to characterize relationships among titanosauriforms (D'Emic, 2012; Mannion et al., 2013). For example, the presence of an elongate (i.e., at least half the functional centrum length) parapophysis in posterior cervical vertebrae and procoelous anterior caudal vertebrae of the D'Emic (2012) analysis would suggest lithostrotian affinities for *Rukwatitan*. Additionally, *Rukwatitan* exhibits the incipient expression of a tubercle on the dorsal margin of the prezygapophysis in the anterior caudal vertebrae and a humerus with a weakly developed posterolateral bulge at the level of the deltopectoral crest, both of which are considered synapomorphies of Saltasauridae (D'Emic, 2012). Similarly,

Mannion et al. (2013) identified other lithostrotian features that are expressed in the *Rukwatitan* materials, including an undivided lateral condyle on the humerus in his standard character (LSDM) analysis and the lack of ventral keel in postaxial cervical centra in his continuous and discrete character (LCDM) analysis. However, it is important to note that both authors primarily focused on relationships of non-titanosaurian titanosauriforms. Although the current data matrix includes 12 titanosaurian taxa, this represents a fraction of the total number (over 50 genera) of potential titanosaurians established to date. Hence, the current study provides a first approximation for establishing the basic phylogenetic affinities of *Rukwatitan*.

DISCUSSION AND CONCLUSIONS

Rukwatitan bisepultus represents an important new taxon for characterizing southern African Cretaceous faunas for two reasons. First, *Rukwatitan* is a prominent member in a relatively new middle Cretaceous African fauna from the Rukwa Rift Basin (RRB) and allows for direct comparisons with the titanosaurian *Malawisaurus dixeyi* from the potentially penecontemporaneous and geographically proximate Dinosaur Beds (DB) of Malawi. The current phylogenetic analyses suggests *Rukwatitan* not as the sister taxon to *Malawisaurus*, but rather as a non-lithostrotian titanosaurian. Taken together, both *Rukwatitan* and *Malawisaurus* form a paraphyletic African grade (although with some ambiguity noted in Phylogenetic Relationships, above). Second, *Rukwatitan* contributes to the characterization of Mesozoic African faunas more generally and facilitates comparisons among southern (i.e., sub-Saharan) and northern (i.e., circum-Saharan) African Cretaceous faunas. The regional biotic similarity hypothesis (O'Connor et al., 2006) posits a significant overlap between the sub-Saharan RRB and the DB faunas, with the sub-Saharan faunas being generally distinct from the circum-Saharan faunas.

The holotype of *Rukwatitan bisepultus* is complete enough to allow a detailed comparison with *Malawisaurus dixeyi* (Jacobs et al., 1993; Gomani, 2005). Based on overall size, *Rukwatitan* appears larger than any of the recovered material of *Malawisaurus.* The maximum centrum lengths of posterior cervical vertebrae and the maximum length of the humerus in *Rukwatitan* are all significantly longer than equivalent elements recovered for *Malawisaurus* (see Table 1 for *Rukwatitan* measurements; see tables 2, 5, and 8 in Gomani [2005] for *Malawisaurus* measurements). For example, the holotype and referred humeri of *Rukwatitan* are approximately 20% and 28% longer, respectively, than the longest of the three reported humeri of *Malawisaurus* (MAL-316; Gomani, 2005:table 7). This may be attributed to differences in ontogenetic stage between the specimens, but the extent of skeletal fusion (e.g., fusion of neural arches and centra along the axial skeleton) within both taxa suggests relatively (skeletally) mature individuals. Additionally, the anterior projection of the cervical rib in *Malawisaurus* extends to the anterior margin of the condyle of the posterior cervical centrum, whereas it only extends to the junction of the condyle and anterior margin of the posterior cervical centrum in *Rukwatitan*. The caudal vertebral series also provide an opportunity for comparative observations. The following features are shared between *Malawisaurus* and *Rukwatitan*: (1) procoelous anterior caudal vertebra; (2) vertebrae that become progressively more amphiplatyan in the middle caudal series; and (3) anterior caudal vertebra with a flat ventral surface (e.g., see MAL-200; Gomani, 1999:fig.1; Gomani, 2005:figs. 14–16). Notable differences between the two taxa include (1) anterior caudal vertebra with an anteroposterior sulcus immediately ventral to the transverse process and middle caudal vertebrae with (2) prominent chevron articular facets; and (3) a ventral longitudinal groove (Gomani, 1999, 2005) in *Malawisaurus*, but not in *Rukwatitan.* Additionally, middle caudal vertebrae of *Malawisaurus* exhibit a prezygapophysis that is nearly parallel along the anteroposterior axis and a dorsally directed neural spine. In contrast, middle caudal vertebrae of *Rukwatitan* possess an anterodorsally projecting prezygapophysis and posterodorsally angled neural spine. Moreover, a number of differences are apparent in the appendicular skeleton between the two taxa. For example, the coracoid of *Rukwatitan* is proximodistally elongate relative to *Malawisaurus* based on the distance between the glenoid and anteroventral corner. The humeri of *Rukwatitan* differ from *Malawisaurus* (MAL-221; Gomani, 2005) in having (1) a more robust proximal end with a well-developed humeral head; (2) a deep coracobrachialis fossa; and (3) a less transversely expanded medial condyle at the distal end. *Malawisaurus* also lacks the prominent posterior protuberance, the lateral bulge, and the subquadrangular midshaft cross-section observed in *Rukwatitan*. Finally, the ulna of *Rukwatitan* has a wider radial fossa than that in *Malawisaurus* (MAL-218; Gomani, 2005:fig. 21). These specific morphological findings are consistent with the results of the phylogenetic analyses conducted herein and support *Rukwatitan* as a distinct taxon from *Malawisaurus*.

Previous preliminary sauropod comparisons between the RRB and DB faunas have included isolated sauropod teeth (RRBP [TNM] 02093; Roberts et al., 2004; Stevens et al., 2008) and isolated procoelous middle caudal vertebrae (RRBP [TNM] 02065, RRBP [TNM] 02072) from locality TZ-07, all of which have been provisionally referred to Titanosauria (O'Connor et al., 2006). Those procoelous middle caudal vertebrae contrast with the morphology observed in both *Rukwatitan* (this contribution) and *Malawisaurus* (Jacobs et al., 1993; Gomani, 1999, 2005), in which the middle caudal vertebrae are amphiplatyan/amphicoelous. Hence, the recovery of procoelous middle caudal centra from the Galula Formation suggests the presence of at least one additional derived titanosaurian in the RRB fauna. It is notable that Gomani (1999) also described two additional types of caudal vertebrae along with the caudal elements of *Malawisaurus dixeyi*. The first type, referred to as 'undesignated morph 1' (MAL-5 from locality CD-4; Gomani, 1999, 2005), is generally similar to the caudal vertebrae described by O'Connor et al. (2006), because both are procoelous middle caudal vertebrae of derived titanosaurian affinities. However, the second vertebral series, referred to as 'undesignated morph 2' (MAL-1, MAL-3, MAL-222, and MAL-230 from locality CD-9, the same bone bed that the holotype of *Malawisaurus* was recovered; Gomani, 1999, 2005), shares some characteristics with *Rukwatitan*. For example, these middle–distal caudal vertebrae are subrectangular, amphicoelous, and exhibit relatively poorly developed chevron facets. However, 'undesignated morph 2' vertebrae also exhibit a weak longitudinal groove on the ventral surface of the centrum and have a vertically oriented neural spine, features not observed in the recovered middle caudal vertebrae of *Rukwatitan*. This seems to suggest that there were, at minimum, four different titanosaurian morphs (i.e., *Malawisaurus*, *Rukwatitan*, 'undesignated morph 1,' 'undesignated morph 2') in sub-Saharan Africa during the middle Cretaceous. How the variation observed in 'undesignated morph 1' and 'undesignated morph 2' from Malawi and the unassigned materials from the RRB relate to either *Rukwatitan* or *Malawisaurus* remains unresolved. Moreover, the way in which these vertebral morphs may be affiliated with the other Dinosaur Beds titanosaurian, *Karongasaurus gittelmani*, also remains unresolved. The holotype of this taxon is based entirely on an isolated dentary and several referred teeth (dentary, MAL-175; teeth, MAL-7, 10–16, 33, 36, 39, 153, 156, 267–269, 271, 272, 307; Gomani, 2005). The teeth associated with *Karongasaurus* are narrow-crowned, with a high-angled wear facet, features typical of derived titanosaurians (Upchurch, 1998; Wilson, 2002; Upchurch et al., 2004) but that differ significantly

from the teeth of *Malawisaurus.* The teeth in the latter form are broad, but not spoon-shaped, with high angle wear facets (Gomani, 2005). The future recovery of better preserved, associated, and articulated materials will allow these issues to be addressed.

Rukwatitan bisepultus adds an important new taxonomic datum to the terrestrial vertebrate record of continental Africa during the middle Cretaceous. The basal titanosaurians *Malawisaurus dixeyi* (Gomani, 2005) and *Rukwatitan* aid in supporting the regional biotic similarity hypothesis put forth by O'Connor et al. (2006) and the more general regional endemism hypothesis (Jacobs et al., 1996) to account for the distribution of terrestrial vertebrate faunas on continental Africa. A similar pattern has been identified in other terrestrial vertebrates, where the closely related notosuchian crocodyliforms *Pakasuchus kapilimai* (O'Connor et al., 2010) and *Malawisuchus mwakasyungutiensis* (Gomani, 1997) together form either a monophyletic grouping or successive outgroups to the exclusion of crocodyliforms from other regions of Africa and Gondwana more generally (O'Connor et al., 2010; Sertich and O'Connor, 2014). Although not included in the present phylogenetic analyses, resolving the relationship of the titanosaurian *Paralititan stromeri* from northern Africa (Smith et al., 2001) would help assess this hypothesis. Only three phylogenetic analyses have included *Paralititan* (Smith et al., 2001; Curry Rogers, 2005; Mannion and Upchurch, 2011). Smith et al. (2001) found *Paralititan* within a totally unresolved titanosaurian clade, and both Curry Rogers (2005) and Mannion and Upchurch (2011) found *Paralititan* as a basal titanosaurian, with the Late Cretaceous *Argyrosaurus* of South America as a sister taxon in some of their reported trees. Additionally, *Malawisaurus* was found to be only distantly related to *Paralititan*, nested within a clade of titanosaurians that preserve cranial material. However, due to the amount of missing data for *Paralititan* and the number of MPTs (approximately 200,000 in Curry Rogers [2005] and 50,000 in the Mannion and Upchurch [2011] reanalysis of her matrix prior to applying reduced consensus efforts) in her most inclusive analysis, Curry Rogers (2005) excluded *Paralititan* and several other problematic taxa (e.g., the destroyed *Aegyptosaurus*) from her more constrained phylogenetic analyses. *Rukwatitan* differs from *Paralititan* in several ways even if the latter is based on fragmentary material. The anterior caudal centrum of *Rukwatitan* is taller than wide, whereas the anterior caudal centrum of *Paralititan* is roughly equal in terms of height and width. Besides being much larger than *Rukwatitan*, the humerus of *Paralititan* is more transversely expanded distally and exhibits well-developed and elongated supracondylar ridges, a strongly sinusoidal proximal surface, an elongated and medially deflected deltopectoral crest, and well-developed anterolateral and anteromedial ridges along the distal half (Smith et al., 2001). Future treatments that include *Paralititan* with additional basal and derived titanosaurians may be able to aid in resolving these regional and paleobiogeographic issues.

The terrestrial vertebrate faunas from the middle Cretaceous of northern Africa are notably different from the growing faunas from southern Africa, particularly with regard to dinosaurian forms. Large-bodied theropods (e.g., spinosaurids, carcharodontosaurids), sauropods (rebacchisaurids, non-titanosaurian titanosauriforms, and rare fragments of titanosaurians), and ornithopods currently characterize middle Cretaceous faunas of northern Africa (Weishampel et al., 2004). With the exception of the titanosaurians, none of the aforementioned dinosaur clades from northern Africa have been identified, described, or reported from middle Cretaceous RRB or DB of sub-Saharan Africa (O'Connor et al., 2006). To properly assess whether this represents a regional paleobiogeographic signal or simply sampling bias requires continued exploration of middle Cretaceous deposits of southern Africa.

ACKNOWLEDGMENTS

We thank D. Kamamba, F. Ndunguru, J. Temba, and J. Temu (Tanzania Antiquities Unit), P. Msemwa (formerly of Tanzania Museum of House of Culture), S. Ngasala, I. Marobhe, and N. Boniface (University of Dar es Salaam), and the Tanzania Commission for Science and Technology (COSTECH) for logistical and administrative support; E. K. Lund, S. Egberts, K. Melstrom, and W. Holloway for assistance with mechanical and digital preparation; members of the 2007 and 2008 Rukwa Rift Basin Project expeditions for field assistance; H. and M. Faessler for continued support in Mbeya; E. Gomani for specimen access in the collections at the Malawi Division of Antiquities; M. D'Emic and M. Carrano for fruitful discussions; J. Sattler (Ohio University Heritage College of Osteopathic Medicine) for photography; and B. Keaner, C. Pugh, and J. Sands (Holzer Clinic, Athens, Ohio) for assistance with computed tomography scanning. M. D'Emic and P. Mannion provided extremely useful reviews of the original submission of this contribution. This research was supported by the U.S. National Science Foundation (NSF EAR 0617561, EAR 0854218, EAR 0933619), the National Geographic Society (CRE), and the Ohio University Heritage College of Osteopathic Medicine and Ohio University Office of Research and Sponsored Programs.

LITERATURE CITED

Allain, R., P. Taquet, B. Battail, J. Dejax, P. Richir, M. Vèra, F. Limon-Duparcmeur, R. Vacant, O. Mateus, P. Sayarath, B. Khenthavong, and S. Phouyavong. 1999. Un nouveau genre de dinosaure sauropode de la formation des Grès supérieurs (Aptien–Albien) du Laos. Comptes Rendus de l'Acadèmie des Sciences Paris, Sciences de la Terre et des planètes 329:609–613.

Apesteguìa, S. 2007. The sauropod diversity of the La Amarga Formation (Barremian), Neuquén (Argentina). Gondwana Research 12: 533–546.

Barrett, P. M., and Upchurch, P. 2005. Sauropod diversity through time: possible macroevolutionary and palaeoecological implications; pp. 125–156 in K. A. Curry Rogers and J. A. Wilson (eds.), The Sauropods: Evolution and Paleobiology. University of California Press, Berkeley, California.

Baumel, J. J., and L. M. Witmer. 1993. Osteologia; pp. 45–132 in J. J. Baumel, A. S. King, J. E. Breazile, H. E. Evans, and J. C. Vanden Berge (eds.), Handbook of Avian Anatomy: Nomina Anatomica Avium. Nuttall Ornithological Club, Cambridge, Massachusetts.

Bellion, Y., J. P. Lefranc, and J.-G. Michard. 1990. Précisions sur l'âge des sédiments méso-cénozoïques á l'ouest de l'Adrar des Iforas (Sahara, Mali, Afrique de l'ouest): implications paléogéograph iques; pp 7–27 in Editions du C.T.H.S. (Paris) (eds.), Actes du Congrès National des Societes Savantes 115, Section des Sciences, 9–12 April 1990, Avignon, France.

Bonaparte, J. F., and R. A. Coria. 1993. Un nuevo y gigantesco saurópodo titanosaurio de la Formación Río Limay (Albiano-Cenomaniano) de la Provincia del Neuquén, Argentina. Ameghiniana 30:271–282.

Bonaparte, J. F., B. J. Gonzalez Riga, and S. Apesteguía. 2006. *Ligabuesaurus leanzai* gen. et sp. nov. (Dinosauria, Sauropoda), a new titanosaur from the Lohan Cura Formation (Aptian, Lower Cretaceous) of Neuquén, Patagonia, Argentina. Cretaceous Research 27:364–376.

Borsuk-Bialynicka, M. 1977. A new camarasaurid sauropod *Opisthocoelicaudia skarzynskii*, gen. n., sp. n. from the Upper Cretaceous of Mongolia. Palaeontologia Polonica 37:5–64.

Broin, F. de, E. Buffetaut, J. C. Koeniguer, J. C. Rage, D. Russell, P. Taquet, C. Vergnaud-Grazzini, and S. Wenz. 1974. La faune de vertébrés continentaux du gisement d'In Beceten (Sénonien du Niger). Comptes Rendus de l'Academie des Sciences Paris 279: 469–472.

Calvo, J. O., and J. F. Bonaparte. 1991. *Andesaurus delgadoi*, gen. et sp. nov. (Saurischia-Sauropoda), dinosaurio Titanosauridae de la Formacíon Río Limay (Albiano-Cenomaniano), Neuquén, Argentina. Ameghiniana 28:303–310.

Calvo, J. O., B. J. González-Riga, and J. D. Porfiri. 2007. A new titanosaur sauropod from the Late Cretaceous of Neuquén, Patagonia, Argentina. Arquivos Do Museu Nacional 65:485–504.

Campos, D. A., and A. W. A. Kellner. 1999. On some sauropod (Titanosauridae) pelves from the continental Cretaceous of Brazil. National Science Museum Monographs 15:143–166.

Campos, D. A., A. W. A. Kellner, R. J. Bertini, and R. M. Santucci. 2005. On a titanosaurid (Dinosauria, Sauropoda) vertebral column from the Bauru group, Late Cretaceous of Brazil. Arquivos Do Museu Nacional 63:565–593.

Carballido, J. L., D. Pol, I. Cerda, and L. Salgado. 2011. The osteology of *Chubutisaurus Insignis* Del Corro, 1975 (Dinosauria: Neosauropoda) from the "middle" Cretaceous of central Patagonia, Argentina. Journal of Vertebrate Paleontology 31:93–110.

Cerda, I. A., L. Salgado, and J. I. E. Powell. 2012a. Extreme postcranial pneumaticity in sauropod dinosaurs from South America. Paläontologische Zeitschrift 86:441–449.

Cerda, I. A., A. P. Carabajal, L. Salgado, R. A. Coria, M. A. Reguero, C. P. Tambussi, and J. J. Moly. 2012b. The first record of a sauropod dinosaur from Antarctica. Naturwissenschaften 99:83–87.

Clarke, J. A., and K. M. Middleton. 2008. Mosaicism, modules, and the evolution of birds: results from a Bayesian approach to the study of morphological evolution using discrete character data. Systematic Biology 57:185–201.

Curry Rogers, K. A. 2005. Titanosauria: a phylogenetic overview; pp. 50–103 in K. A. Curry Rogers and J. A. Wilson (eds.), The Sauropods: Evolution and Paleobiology. University of California Press, Berkeley, California.

Curry Rogers, K. A. 2009. The postcranial osteology of *Rapetosaurus krausei* (Sauropoda: Titanosauria) from the Late Cretaceous of Madagascar. Journal of Vertebrate Paleontology 29:1046–1086.

D'Emic, M. D. 2012. The early evolution of titanosauriform sauropod dinosaurs. Zoological Journal of the Linnean Society 166:624–671.

D'Emic, M. D., and J. A. Wilson. 2012. Bone histology of a dwarf sauropod dinosaur from the latest Cretaceous of Jordan and a possible biomechanical explanation for "titanosaur-type" bone histology. Journal of Vertebrate Paleontology, Program and Abstracts 2012:83A.

del Corro, G. 1975. Un nuevo saurópodo del Cretácico *Chubutisaurus insignis* gen. et sp. nov. (Saurischia-Chubutisauridae nov.) del Cretácico Superior (Chubutiano), Chubut, Argentina, 12–16 August 1974; pp. 229–240 in Actas I Congreso Argentino de Paleontología y Bioestratigrafía, Tucuman, Volume 2, Asociación Paleontológica Argentina, Tucumán, Argentina.

Dong, Z. 1990. Sauropoda from the Kelameili region of the Junggar basin, Xinjiang autonomous region. Vertebrata PalAsiatica 28:43–58.

Farris, J. S., V. A. Albert, M. Kallersjo, D. Lipscomb, and A. G. Kluge. 1996. Parsimony jackknifing outperforms neighbor-joining. Cladistics 12:99–124.

Felsenstein, J. 1985. Confidence-limits on phylogenies—an approach using the bootstrap. Evolution 39:783–791.

Gomani, E. M. 1997. A crocodyliform from the Early Cretaceous Dinosaur Beds, northern Malawi. Journal of Vertebrate Paleontology 17:280–294.

Gomani, E. M. 1999. Sauropod caudal vertebrae from Malawi, Africa; pp. 235–248 in Y. Tomida, T. H. Rich, and P. Vickers-Rich (eds.), Proceedings of the Second Gondwanan Dinosaur Symposium, 12–13 July 1998. National Science Museum Monographs 15, Tokyo, Japan.

Gomani, E. M. 2005. Sauropod dinosaurs from the Early Cretaceous of Malawi, Africa. Palaeontologia Electronica 8(1):27A. Available at http://palaeo-electronica.org/2005_1/gomani27/issue1_05.htm. Accessed May 2, 2011.

Greigert, J., F. Joulia, and A. F. de Lapparent. 1954. Répartition stratigraphique des gisements de vertebrés dans le crétacé du Niger. Comptes Rendus Hebdomadaires des Seances de l'Academie des Sciences 239:433–435.

Hocknull, S. A., M. A. White, T. R. Tischler, A. G. Cook, N. D. Calleja, T. Sloan, and D. A. Elliot. 2009. New mid-Cretaceous (latest Albian) dinosaurs from Winton, Queensland, Australia. PLoS ONE 4:e6190. doi: 10.1371/journal.pone.0006190.

Huelsenbeck, J. P., and F. Ronquist. 2001. MRBAYES: Bayesian inference of phylogeny. Bioinformatics 17:754–755.

Jacobs, L. L., D. A. Winkler, and E. M. Gomani. 1996. Cretaceous dinosaurs from Africa: examples from Cameroon and Malawi. Memoirs of the Queensland Museum 39:595–610.

Jacobs, L. L., D. A. Winkler, W. R. Downs, and E. M. Gomani. 1993. New material of an Early Cretaceous titanosaurid sauropod dinosaur from Malawi. Palaeontology 36:523–534.

Juárez Valieri, R. D., J. O. Calvo, J. O. Calvo, J. D. Porfiri, B. J. González Riga, and D. D. Santos. 2011. Revision of MUCPv 204, a Senonian basal titanosaur from northern Patagonia; pp. 143–152 in J. O. Calvo, J. D. Porfiri, B. J. González Riga, and D. Dos Santos (eds.), Dinosaurios y Paleontología Desde América Latina, Editorial de la Universidad Nacional de Cuyo, Mendoza, Argentina.

Kass, R. E., and A. E. Raftery. 1995. Bayes Factors. Journal of the American Statistical Association 90:773–795.

Kear, B. P., and P. M. Barrett. 2011. Reassessment of the Lower Cretaceous (Barremian) pliosauroid *Leptocleidus superstes* Andrews, 1922 and other plesiosaur remains from the nonmarine Wealden succession of southern England. Zoological Journal of the Linnean Society 161:663–691.

Kellner, A. W. A., and S. A. K. Azevedo. 1999. A new sauropod dinosaur (Titanosauria) from the Late Cretaceous of Brazil. National Science Museum Monographs 15:111–142.

Kellner, A. W. A., D. A. Campos, and M. N. Trotta. 2005. Description of a titanosaurid caudal series from the Bauru Group, Late Cretaceous of Brazil. Arquivos Do Museu Nacional 63:529–564.

Kennedy, W. J., H. C. Klinger, and N. J. Mateer. 1987. First record of an Upper Cretaceous sauropod dinosaur from Zululand, South Africa. South African Journal of Science 83:173–174.

Krause, D. W., S. D. Sampson, M. T. Carrano, and P. M. O'Connor. 2007. Overview of the history of discovery, taxonomy, phylogeny, and biogeography of *Majungasaurus crenatissimus* (Theropoda: Abelisauridae) from the Late Cretaceous of Madagascar. Journal of Vertebrate Paleontology 27:1–20.

Krause, D. W., P. M. O'Connor, K. C. Rogers, S. D. Sampson, G. A. Buckley, and R. R. Rogers. 2006. Late Cretaceous terrestrial vertebrates from Madagascar: implications for Latin American biogeography. Annals of the Missouri Botanical Garden 93:178–208.

Lapparent, A. F. de. 1960. Les dinosauriens du "Continental Intercalaire" du Sahara Central. Mémoire de la Societé Géologique de France 88A:1–57.

Leanza, H. A., S. Apesteguıa, F. E. Novas, and M. S. de la Fuente. 2004. Cretaceous terrestrial beds from the Neuquén Basin (Argentina) and their tetrapod assemblages. Cretaceous Research 25:61–87.

Lee, M. S. Y. 2005. Molecular evidence and marine snake origins. Biology Letters 1:227–230.

Lee, M. S. Y., and T. H. Worthy. 2012. Likelihood reinstates *Archaeopteryx* as a primitive bird. Biology Letters 8:299–303.

Lewis, P. O. 2001. A likelihood approach to estimating phylogeny from discrete morphological character data. Systematic Biology 50:913–925.

Maddison, W. P., and D. R. Maddison. 2011. Mesquite: A Modular System for Evolutionary Analysis, version 2.75. Available at http://mesquiteproject.org. Accessed January 1, 2013.

Magallón, S. 2010. Using fossils to break long branches in molecular dating: a comparison of relaxed clocks applied to the origin of angiosperms. Systematic Biology 59:384–399.

Mannion, P. D. 2011. A reassessment of *Mongolosaurus haplodon* Gilmore, 1933, a titanosaurian sauropod dinosaur from the Early Cretaceous of Inner Mongolia, People's Republic of China. Journal of Systematic Palaeontology 9:355–378.

Mannion, P. D., and J. O. Calvo. 2011. Anatomy of the basal titanosaur (Dinosauria, Sauropoda) *Andesaurus delgadoi* from the mid-Cretaceous (Albian-early Cenomanian) Río Limay Formation, Neuquén Province, Argentina: implications for titanosaur systematics. Zoological Journal of the Linnean Society 163:155–181.

Mannion, P. D., and A. Otero. 2012. A reappraisal of the Late Cretaceous Argentinean sauropod dinosaur *Argyrosaurus superbus*, with a description of a new titanosaur genus. Journal of Vertebrate Paleontology 32:614–638.

Mannion, P. D., and P. Upchurch. 2011. A re-evaluation of the mid-Cretaceous sauropod hiatus and the impact of uneven sampling of the fossil record on patterns of regional dinosaur extinction. Palaeogeography, Palaeoclimatology, Palaeoecology 299:529–540.

Mannion, P. D., P. Upchurch, R. N. Barnes, and O. Mateus. 2013. Osteology of the Late Jurassic Portuguese sauropod dinosaur *Lusotitan atalaiensis* (Macronaria) and the evolutionary history of basal titanosauriforms. Zoological Journal of the Linnean Society 168:98–206.

Mannion, P. D., P. Upchurch, O. Mateus, R. N. Barnes, and M. E. H. Jones. 2012. New information on the anatomy and systematic

position of *Dinheirosaurus lourinhanensis* (Sauropoda: Diplodocoidea) from the Late Jurassic of Portugal, with a review of European diplodocoids. Journal of Systematic Palaeontology 10:521–551.
Marsh, O. C. 1878. Principal characters of American Jurassic dinosaurs. Part I. American Journal of Science, Series 3 16:411–416.
Martínez, R., O. Gimenez, J. Rodriguez, M. Luna, and M. Lamanna. 2004. An articulated specimen of the basal titanosaurian (Dinosauria: Sauropoda) *Epachthosaurus sciuttoi* from the early Late Cretaceous Bajo Barreal Formation of Chubut Province, Argentina. Journal of Vertebrate Paleontology 24:107–120.
Mateus, O., L. L. Jacobs, A. S. Schulp, M.J. Polcyn, T. S. Tavares, A. B. Neto, M. L. Morais, and M. T. Antunes. 2011. *Angolatitan adamastor*, a new sauropod dinosaur and the first record from Angola. Anais da Academia Brasileirade Ciências 83:221–233.
Moody, R., and P. Sutcliffe. 1990. Cretaceous-Tertiary crossroads of migration in the Sahel. Geology Today 6:19–23.
Müller, J., and R. Reisz. 2006. The phylogeny of early eureptiles: comparing parsimony and Bayesian approaches in the investigation of a basal fossil clade. Systematic Biology 55:503–511.
Novas, F. E. 2009. The Age of Dinosaurs in South America. Indiana University Press, Bloomington and Indianapolis, Indiana, 452 pp.
Nylander, J., F. Ronquist, J. Huelsenbeck, and J. Nieves-Aldrey. 2004. Bayesian phylogenetic analysis of combined data. Systematic Biology 53:47–67.
O'Connor P., M. Gottfried, N. Stevens, E. Roberts, S. Ngasala, S. Kapilima, and R. Chami. 2006. A new vertebrate fauna from the Cretaceous Red Sandstone Group, Rukwa Rift Basin, Southwestern Tanzania. Journal of African Earth Sciences 44:277–288.
O'Connor, P. M., J. J. W. Sertich, N. J. Stevens, E. M. Roberts, M. D. Gottfried, T. L. Hieronymus, Z. A. Jinnah, R. Ridgely, S. E. Ngasala, and J. Temba. 2010. The evolution of mammal-like crocodyliforms in the Cretaceous Period of Gondwana. Nature 466:748–751.
O'Leary, M., E. Roberts, J. Head, F. Sissoko, and M. Bouare. 2004. Titanosaurian (Dinosauria: Sauropoda) remains from the "Continental Intercalaire" of Mali. Journal of Vertebrate Paleontology 24:923–930.
Owen, R. 1842. Report on British fossil reptiles, Part II. Reports of the British Association for the Advancement of Science 11:60–204.
Powell, J. E. 1990. *Epachthosaurus sciuttoi* (gen. et sp. nov.) un dinosaurio sauropodo del Cretacico de Patagonia (Provincia de Chubut, Argentina); pp. 123–128 in Congreso Argentino de Paleontologia y Bioestratigradia, Tucuman, Actas 1, Universidad Nacional de Tucumán, Instituto Superior de Correlación Geológica, Tucumán, Argentina.
Prieto-Márquez, A. 2010. Global phylogeny of hadrosauridae (Dinosauria: Ornithopoda) using parsimony and Bayesian methods. Zoological Journal of the Linnean Society 159:435–502.
Pyron, R. A. 2011. Divergence time estimation using fossils as terminal taxa and the origins of Lissamphibia. Systematic Biology 60: 466–481.
Rauhut, O. W. M., K. Remes, R. Fechner, G. Cladera, and P. Puerta. 2005. Discovery of a short-necked sauropod dinosaur from the Late Jurassic period of Patagonia. Nature 435:670–672.
Roberts, E., P. O'Connor, M. Gottfried, N. Stevens, S. Kapalima, and S. Ngasala. 2004. Revised stratigraphy and age of the Red Sandstone Group in the Rukwa Rift Basin, Tanzania. Cretaceous Research 25:749–759.
Roberts, E. M., P. M. O'Connor, N. J. Stevens, M. D. Gottfried, Z. A. Jinnah, S. Ngasala, A. M. Choh, and R. A. Armstrong. 2010. Sedimentology and depositional environments of the Red Sandstone Group, Rukwa Rift Basin, southwestern Tanzania: new insight into Cretaceous and Paleogene terrestrial ecosystems and tectonics in sub-equatorial Africa. Journal of African Earth Sciences 57: 179–212.
Roberts, E. M., N. J. Stevens, P. M. O'Connor, P. H. G. M. Dirks, M. D. Gottfried, W. C. Clyde, R. A. Armstrong, A. I. S. Kemp, and S. Hemming. 2012. Initiation of the western branch of the East African Rift coeval with the eastern branch. Nature Geoscience 5:289–294.
Ronquist, F., and J. P. Huelsenbeck. 2003. MrBayes 3: Bayesian phylogenetic inference under mixed models. Bioinformatics 19:1572–1574.
Ronquist, F., S. Klopfstein, L. Vilhelmsen, S. Schulmeister, D. L. Murray, and A. P. Rasnitsyn. 2012. A total-evidence approach to dating with fossils, applied to the early radiation of the Hymenoptera. Systematic Biology 61:973–999.
Royo-Torres, R., A. Cobos, and L. Alcala. 2006. A giant European dinosaur and a new sauropod clade. Science 314:1925–1927.
Salgado, L., and J. F. Bonaparte. 1991. Un nuevo sauropodo Dicraeosauridae, *Amargasaurus cazaui*, gen. et sp. nov., de la Formación La Amarga, Neocomiano de la Provincia del Neuquen, Argentina. Ameghiniana 28:333–346.
Salgado, L., and J. F. Bonaparte. 2007. Sauropodomorpha; pp. 188–228 in Z. Gasparini, L. Salgado, and R. A. Coria (eds.), Patagonian Mesozoic Reptiles. Indiana University Press, Bloomington and Indianapolis, Indiana.
Salgado, L., S. Apesteguía, and S. E. Heredia. 2005. A new specimen of *Neuquensaurus australis*, a Late Cretaceous saltasaurine titanosaur from North Patagonia. Journal of Vertebrate Paleontology 25:623–634.
Salgado, L., R. A. Coria, and J. O. Calvo. 1997. Evolution of titanosaurid sauropods: phylogenetic analysis based on the postcranial evidence. Ameghiniana 34:3–32.
Sanz, J. L., J. E. Powell, J. Le Loeuff, R. Martinez, and X. Pereda Suberbiola. 1999. Sauropod remains from the Upper Cretaceous of Laño (northcentral Spain). Titanosaur phylogenetic relationships. Estudios Del Museo De Ciencias Naturales De Alava 14:235–255.
Seeley, H. G. 1887. On the classification of the fossil animals commonly named Dinosauria. Proceedings of the Royal Society of London 43:165–171.
Sereno, P. C. 1999. The evolution of dinosaurs. Science 284:2137–2147.
Sereno, P. C., and S. L. Brusatte. 2008. Basal abelisaurid and carcharodontosaurid theropods from the Lower Cretaceous Elrhaz Formation of Niger. Acta Palaeontologica Polonica 53:15–46.
Sereno, P. C., J. A. Wilson, and J. L. Conrad. 2004. New dinosaurs link southern landmasses in the mid-Cretaceous. Proceedings of the Royal Society of London, Series B 271:1325–1330.
Sereno, P. C., J. A. Wilson, L. M. Witmer, J. A. Whitlock, A. Maga, O. Ide, and T. A. Rowe. 2007. Structural extremes in a Cretaceous dinosaur. PLoS ONE 2:e1230. doi: 10.1371/journal.pone.0001230.
Sereno, P. C., A. Beck, D. Dutheil, H. Larsson, G. Lyon, B. Moussa, R. Sadleir, C. Sidor, D. Varricchio, G. Wilson, and J. Wilson. 1999. Cretaceous sauropods from the Sahara and the uneven rate of skeletal evolution among dinosaurs. Science 286:1342–1347.
Sertich, J. J. W., and P. M. O'Connor. 2014. A new crocodyliform from the middle Cretaceous Galula Formation, southwestern Tanzania. Journal of Vertebrate Paleontology 34:576–596.
Smith, J. B., M. C. Lamanna, K. J. Lacovara, P. Dodson, J. R. Smith, J. C. Poole, R. Giegengack, and Y. Attia. 2001. A giant sauropod dinosaur from an Upper Cretaceous mangrove deposit in Egypt. Science 292:1704–1706.
Snively, E., and A. Cox. 2008. Structural mechanics of pachycephalosaur crania permitted head-butting behavior. Palaeontologia Electronica 11(1):3A. Available at http://palaeo-electronica.org/2008_1/140/. Accessed May 2, 2011.
Stevens, N. J., M. D. Gottfried, E. M. Roberts, S. Ngasala, S. Kapilima, and P. M. O'Connor. 2008. Paleontological exploration in Africa: a view from the Rukwa Rift Basin of Tanzania; pp. 159–180 in E. Simons (ed.), A Search for Origins, Developments in Primatology: Progress and Prospects. Springer Science+Business Media, New York.
Stromer, E. 1932. Wirbeltierreste der Baharije-Stufe (unterstes Cenoman). 11. Sauropoda. Abhandlungen der Bayerischen Akademie der Wissenschaften, Mathematisch-Naturwissenschaftliche Abteilung 10:1–21.
Suteethorn, S., J. Le Loeuff, E. Buffetaut, V. Suteethorn, C. Talubmook, and C. Chonglakmani. 2009. A new skeleton of *Phuwiangosaurus sirindhornae* (Dinosauria, Sauropoda) from NE Thailand; pp. 189–215 in E. Buffetaut, G. Cuny, J. Le Loeff, and V. Suteethorn (eds.), Late Paleozoic and Mesozoic Ecosystems in Southeast Asia. Special Publication of the Geological Society of London 315.
Swofford, D. L. 2003. PAUP*: Phylogenetic Analysis Using Parsimony (*And Other Methods), version 4. Sinauer Associates, Sunderland, Massachusetts.
Upchurch, P. 1995. The evolutionary history of sauropod dinosaurs. Philosophical Transactions of the Royal Society of London, Series B 349:365–390.
Upchurch, P. 1998. The phylogenetic relationships of sauropod dinosaurs. Zoological Journal of the Linnean Society 124:43–103.
Upchurch, P. 1999. The phylogenetic relationships of the Nemegtosauridae (Saurischia, Sauropoda). Journal of Vertebrate Paleontology 19:106–125.

Upchurch, P., and P. M. Barrett. 2005. A phylogenetic perspective on sauropod diversity; pp. 104–124 in K. A. Curry Rogers and J. A. Wilson (eds.), The Sauropods: Evolution and Paleobiology. University of California Press, Berkeley, California.

Upchurch, P., P. M. Barrett, and P. Dodson. 2004. Sauropoda; pp. 259–322 in D. B. Weishampel, P. Dodson, and H. Osmólska (eds.), The Dinosauria, second edition. University of California Press, Berkeley, California.

Wedel, M. J. 2003. Vertebral pneumaticity, air sacs, and the physiology of sauropod dinosaurs. Paleobiology 29:243–255.

Wedel, M. J., and R. K. Sanders. 2002. Osteological correlates of cervical musculature in Aves and Sauropoda (Dinosauria: Saurischia), with comments on the cervical ribs of *Apatosaurus*. PaleoBios 22 (3):1–6.

Weishampel, D. B., P. M. Barrett, R. A. Coria, J. Le Loeuff, X. Xing, X.-J. Zhao, A. Sahni, E. M. Gomani, and C. R. Noto. 2004. Dinosaur distributions; pp. 517–606 in D. B. Weishampel, P. Dodson, and H. Osmólska (eds.), The Dinosauria, second edition. University of California Press, Berkeley, California.

Whitlock, J. A. 2011. A phylogenetic analysis of Diplodocoidea (Saurischia: Sauropoda). Zoological Journal of the Linnean Society 161:872–915.

Wiens, J. J., R. Bonett, and P. Chippindale. 2005. Ontogeny discombobulates phylogeny: paedomorphosis and higher-level salamander relationships. Systematic Biology 54:91–110.

Wiens, J. J., C. A. Kuczynski, T. Townsend, T. W. Reeder, D. G. Mulcahy, and J. W. Sites. 2010. Combining phylogenomics and fossils in higher-level squamate reptile phylogeny: molecular data change the placement of fossil taxa. Systematic Biology 59:674–688.

Wilson, J. A. 2002. Sauropod dinosaur phylogeny: critique and cladistic analysis. Zoological Journal of the Linnean Society 136: 217–276.

Wilson, J. A. 2005. Overview of sauropod phylogeny and evolution; pp. 15–49 in K. A. Curry Rogers and J. A. Wilson (eds.), The Sauropods: Evolution and Paleobiology. University of California Press, Berkeley, California.

Wilson, J. A. 2006. An overview of titanosaur evolution and phylogeny; pp. 169–190 in Actas de las III Jornadas Sobre Dinosaurios y Su Entorno, Burgos, September 2004. Colectivo Arqueológico-Paleontológico de Salas, C.A.S.

Wilson, J. A. 2012. New vertebral laminae and patterns of serial variation in vertebral laminae of sauropod dinosaurs. Contributions from the Museum of Paleontology, University of Michigan 32: 91–110.

Wilson, J. A., and P. C. Sereno. 1998. Early evolution and higher-level phylogeny of sauropod dinosaurs. Society of Vertebrate Paleontology Memoir 5:1–68.

Wilson, J. A., and P. Upchurch. 2003. A revision of *Titanosaurus* Lydekker (Dinosauria; Sauropoda), the first dinosaur genus with a Gondwanan distribution. Journal of Systematic Palaeontology 1:125–160.

Wilson, J. A., and P. Upchurch. 2009. Redescription and reassessment of the phylogenetic affinities of *Euhelopus zdanskyi* (Dinosauria: Sauropoda) from the Early Cretaceous of China. Journal of Systematic Paleontology 7:199–239.

Wilson, J. A., M. D. D'Emic, T. Ikejiri, E. M. Moacdieh, and J. A. Whitlock. 2011. A nomenclature for vertebral fossae in sauropods and other saurischian dinosaurs. PLoS ONE 6:e17114. doi: 10.1371/journal.pone.0017114.

Wood, H. M., N. J. Matzke, R. G. Gillespie, and C. E. Griswold. 2013. Treating fossils as terminal taxa in divergence time estimation reveals ancient vicariance patterns in the palpimanoid spiders. Systematic Biology 62:264–284.

Woodward, H. N., and T. M. Lehman. 2009. Bone histology and microanatomy of *Alamosaurus sanjuanensis* (Sauropoda: Titanosauria) from the Maastrichtian of Big Bend National Park, Texas. Journal of Vertebrate Paleontology 29:807–821.

Young, C. C. 1954. On a new sauropod from Yibin, Szeichuan, China. Acta Scientia Sinica 3:491–504.

Xu, X., X. Zhang, Q. Tan, X. Zhao, and L. Tan. 2006. A new titanosaurian sauropod from Late Cretaceous of Nei Mongol, China. Acta Geologica Sinica (English Edition) 80:20–26.

Zaher, H., D. Pol, A. B. Carvalho, P. M. Nascimento, C. Riccomini, P. Larson, R. Juárez-Valieri, R. Pires-Domingues, N. J. da Silva Jr., and D. de Almeida Campos. 2011. A complete skull of an Early Cretaceous sauropod and the evolution of advanced titanosaurians. PLoS ONE 6:e16663. doi: 10.1371/journal.pone.0016663.

Submitted April 19, 2013; revisions received July 19, 2013; accepted September 13, 2013.

Handling editor: Hailu You.